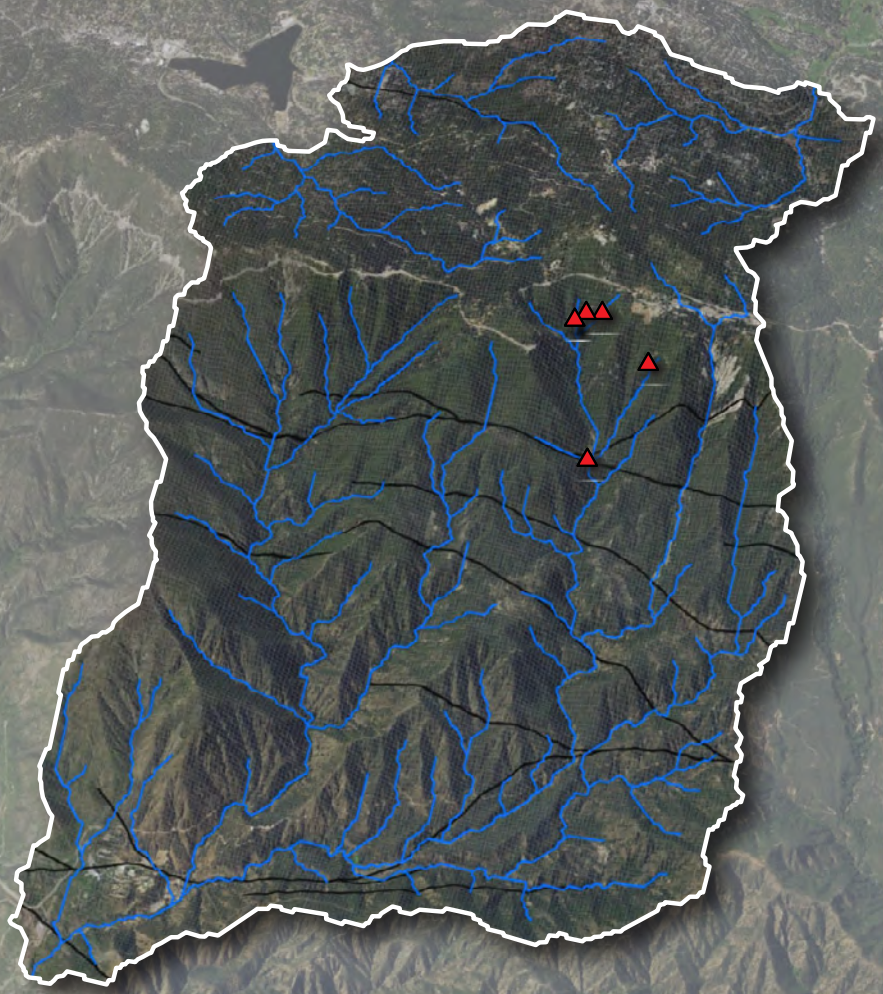
USGS
science for a changing world

Water Resources Mission Area—Water Availability and Use Science Program

Simulation of the Impacts of Spring Diversions on Streamflow in the Strawberry Creek Watershed, San Bernardino County, California, Using an Integrated Hydrological Model



Scientific Investigations Report 2026–5040
Supersedes preprint https://doi.org/10.31223/X5JB2K

U.S. Department of the Interior
U.S. Geological Survey

Cover. The Strawberry Creek watershed (outlined in yellow). The black lines are faults, the black outline is the model active area, red symbols are Arrowhead Springs diversion structures, blue lines are streams, and the small squares are model cells. Orthophotograph by the U.S. Geological Survey National Map.

Simulation of the Impacts of Spring Diversions on Streamflow in the Strawberry Creek Watershed, San Bernardino County, California, Using an Integrated Hydrological Model

By Derek W. Ryter, Joseph A. Hevesi, and Linda R. Woolfenden

Water Resources Mission Area—Water Availability and Use Science Program

Scientific Investigations Report 2026–5040
Supersedes preprint https://doi.org/10.31223/X5JB2K

U.S. Department of the Interior
U.S. Geological Survey

U.S. Geological Survey, Reston, Virginia: 2026
Supersedes preprint https://doi.org/10.31223/X5JB2K

For more information on the USGS—the Federal source for science about the Earth, its natural and living resources, natural hazards, and the environment—visit https://www.usgs.gov.

For an overview of USGS information products, including maps, imagery, and publications, visit https://store.usgs.gov/ or contact the store at 1–888–275–8747.

Any use of trade, firm, or product names is for descriptive purposes only and does not imply endorsement by the U.S. Government.

Although this information product, for the most part, is in the public domain, it also may contain copyrighted materials as noted in the text. Permission to reproduce copyrighted items must be secured from the copyright owner.

Suggested citation:
Ryter, D.W., Hevesi, J.A., and Woolfenden, L.R., 2026, Simulation of the impacts of spring diversions on streamflow in the Strawberry Creek watershed, San Bernardino County, California, using an integrated hydrological model: U.S. Geological Survey Scientific Investigations Report 2026–5040, 30 p., https://doi.org/10.3133/sir20265040. [Supersedes preprint https://doi.org/10.31223/X5JB2K.]

Associated data for this publication:
Ryter, D.W., 2025, Integrated hydrological model for simulating the impacts of spring diversions on streamflow in the Strawberry Creek watershed, San Bernardino County, California: U.S. Geological Survey data release, https://doi.org/10.5066/P13AN2RJ.

ISSN 2328-0328 (online)

Acknowledgments

Valuable assistance was provided by the San Bernardino Valley Water District and the San Bernardino National Forest. Valuable assistance with model development and calibration also was provided by Richard Niswonger of the U.S. Geological Survey.

Contents

Acknowledgments iii
Abstract 1
Purpose and Scope 1
Introduction 1
Study Area Description 4
Hydrogeology and Groundwater Flow 4
Sources of Recharge 7
Mechanisms of Discharge 7
    Natural Discharge 7
    Spring Diversion Structures 7
    Pumpage 9
Watershed Characteristics 11
Streamflow 12
Strawberry Creek Integrated Hydrological Model 13
    Boundaries and Model Discretization 13
        Simulating Spring Diversion Structures 14
        Horizontal Flow Barriers 14
    Precipitation-Runoff Model System 14
    MODFLOW Model 15
        Parameter Zones 17
    Model Calibration 17
        PRMS Calibration 17
        GSFLOW Calibration 20
            Calibrated Parameter Values 21
        Calibration Results 21
Streamflow Capture by the Spring Diversion Structures 24
Discussion and Conclusions 26
    Model Limitations 26
Summary 27
References Cited 28

Figures

1. Map showing location of the study area, watersheds within the study area, Strawberry Creek subdrainages, Arrowhead Springs and diversion structures, municipal wells, weather station, town of Rimforest, streamflow-gaging stations, and recharge area in San Bernardino County, California 3
2. Map showing Strawberry Creek Integrated Hydrological Model extent, watersheds, model cells, layer 1 parameter zones, fault horizontal flow barriers, spring diversions, general head boundary cells, confluence virtual gage, and simulated streams and detail of local Arrowhead Springs area with simulated stream leakage to the aquifer and gain from groundwater, San Bernardino County, California....6
3. Time series plots of simulated and measured spring diversion flow rate for individual spring diversion complexes and the combined spring diversion flow with total annual precipitation, Strawberry Creek Integrated Hydrological Model, San Bernardino County, California 8
4. Graphs of total estimated annual pumpage in the Crestview Water District service area and regression used to estimate the annual domestic pumpage in the Strawberry Creek Integrated Hydrological Model, San Bernardino County, California....10
5. Map showing land cover with vegetation types for the Strawberry Creek study area, San Bernardino County, California 11
6. Bar chart showing mean monthly streamflow measured at the East Twin Creek streamflow-gaging station near Arrowhead Springs, streamflow-gaging station 11058500, period of record 1981–2021, and base flow calculated using the HYSEP hydrograph-separation method with the base-flow index, San Bernardino County, California....13
7. Map showing locations of weather stations managed by the California Irrigation Management Information System, Remote Automatic Weather Stations, San Bernardino County, and the Western Regional Climate Center, used to calculate precipitation and temperature for climate input data for the Strawberry Creek Integrated Hydrological Model, San Bernardino County, California....15
8. Maps showing mean annual interpolated precipitation, snowfall, precipitation and runoff model system simulated infiltration, and Hortonian and Dunnian surface runoff for the Strawberry Creek and adjacent watersheds, Strawberry Creek Integrated Hydrological Model, San Bernardino County, California....16
9. Graph showing simulated and measured monthly mean potential evapotranspiration for the Lake Arrowhead climate station and the nearest model cell, Strawberry Creek Integrated Hydrological Model, San Bernardino County, California....18
10. Graphs showing simulated and measured monthly streamflow used for model calibration with Nash-Sutcliffe efficiency coefficient for East Twin Creek near Arrowhead Springs, U.S. Geological Survey streamflow-gaging station 11058500, and Abondigas Creek at Crestline, U.S. Geological Survey streamflow-gaging station 10260630, Strawberry Creek Integrated Hydrological Model, San Bernardino County, California....19
11. Maps showing model layer 1 hydraulic parameters zones and calibrated values for horizontal hydraulic conductivity, horizontal anisotropy, horizontal flow barrier hydraulic characteristic, and specific yield parameters used in the Strawberry Creek Integrated Hydrological Model, San Bernardino County, California....22

12. Maps showing layer 2 calibrated hydraulic parameters zones and calibrated values for horizontal hydraulic conductivity, horizontal anisotropy, horizontal flow barrier hydraulic characteristic, and specific yield parameters used in the Strawberry Creek Integrated Hydrological Model, San Bernardino County, California 23
13. Scatter plot showing observed groundwater levels and simulated hydraulic heads with a linear regression line, Strawberry Creek Integrated Hydrological Model, San Bernardino County, California 24
14. Bar graph showing total annual precipitation and time-series plots showing simulated mean monthly streamflow with and without spring diversions operating, and mean annual spring diversion flow, and stream loss time series and mean stream loss for Strawberry Creek at the location referred to as the confluence virtual gage, Strawberry Creek Integrated Hydrological Model, San Bernardino County, California 25

Table

1. Ranges and mean annual area-averaged flow in inches for the entire Strawberry Creek Integrated Hydrological Model active area, San Bernardino County, California 20

Conversion Factors

U.S. customary units to International System of Units

Multiply	By	To obtain
	Length	
inch (in.)	2.54	centimeter (cm)
inch (in.)	25.4	millimeter (mm)
foot (ft)	0.3048	meter (m)
mile (mi)	1.609	kilometer (km)
	Area	
square foot (ft^2)	929.0	square centimeter (cm^2)
square foot (ft^2)	0.09290	square meter (m^2)
	Volume	
cubic foot (ft^3)	28.32	cubic decimeter (dm^3)
	Flow rate	
cubic foot per second (ft^3/s)	0.02832	cubic meter per second (m^3/s)
	Hydraulic conductivity	
foot per day (ft/d)	0.3048	meter per day (m/d)

Temperature in degrees Celsius (°C) may be converted to degrees Fahrenheit (°F) as follows:

$$°F = (1.8 \times °C) + 32.$$

Temperature in degrees Fahrenheit (°F) may be converted to degrees Celsius (°C) as follows:

$$°C = (°F - 32) / 1.8.$$

Datum

Vertical coordinate information is referenced to the North American Vertical Datum of 1988 (NAVD 88).

Abbreviations

BFI	base-flow index
CIMIS	California Irrigation Management Information System
CVWD	Crestline Village Water District
ET	evapotranspiration
GSFLOW	groundwater and surface-water flow model
HANI	horizontal anisotropy
HFB	horizontal flow barrier
HK	horizontal hydraulic conductivity
HRU	hydrological response unit
HYDCHR	hydraulic characteristic
MODFLOW	Modular Ground-Water Flow Model
PET	potential evapotranspiration
PPT	precipitation
PRISM	Parameter-elevation Regressions on Independent Slopes Model
PRMS	precipitation-runoff model system
RMSE	root mean square error
SCIHM	Strawberry Creek integrated hydrological model
SDF	stream-depletion factor
SFR	streamflow routing
SS	specific storage
SY	specific yield
USGS	U.S. Geological Survey
VKA	vertical hydraulic conductivity

Simulation of the Impacts of Spring Diversions on Streamflow in the Strawberry Creek Watershed, San Bernardino County, California, Using an Integrated Hydrological Model

By Derek W. Ryter,[1] Joseph A. Hevesi,[2] and Linda R. Woolfenden[2]

Abstract

The Strawberry Creek watershed, in the San Bernardino Mountains of southern California, features a group of natural springs known as Arrowhead Springs that have been augmented with diversions in the form of sub-horizontal borings and tunnels. Understanding the effects of these structures on streamflow through groundwater capture is crucial for managing surface-water resources in this watershed. In this study, we constructed the Strawberry Creek integrated hydrological model to increase this understanding. The Strawberry Creek integrated hydrological model is an integrated surface runoff and groundwater model, GSFLOW to simulate surface runoff and infiltration and groundwater flow. The model has 263 rows and 176 columns in each of its three layers. The model area includes the Strawberry Creek and four adjacent watersheds. The precipitation-runoff modeling system was calibrated using two streamflow gaging stations, and the groundwater and surface-water flow model was calibrated to the reported spring diversion discharge and a sparse number of groundwater-level measurements. The Strawberry Creek integrated hydrological model was run with and without diversions active, and simulated streamflow was compared, indicating that in the headwaters of Strawberry Creek, about 35 percent of the diversion flow was captured from base flow.

Purpose and Scope

The purpose of this report is to present the results of a simulation of the hydrological system of the Strawberry Creek watershed area using an integrated hydrological model to determine the effects of spring diversion structures on streamflow in upper Strawberry Creek. The model simulated the surface and groundwater system calibrated to spring diversion discharge. The simulated streamflow with and without the spring diversions was compared to determine how much of the diversion discharge was groundwater captured from base flow to Strawberry Creek.

Introduction

Headwater streams serve as the initial channels where surface runoff and snowmelt begin to accumulate and flow downstream. They provide an important source of streamflow to watersheds in semiarid regions because of increased precipitation in higher elevations. Runoff can be highly seasonal because of temporal precipitation patterns and extended dry seasons, but base flow and spring discharge from groundwater can help to sustain streamflow during times of deficit. Groundwater discharge to springs and streams is also closely tied to groundwater levels, which are sensitive to the water balance between recharge and discharge. The rate of groundwater discharge to streams in headwater basins is typically low but is nonetheless vital to stream and riparian habitat (Meyer and others, 2007; Roy and others, 2011; Springer and others, 2015). Thus, for protection of riverine habitat, it is important to understand the interplay between all components of the hydrological system and the effects of groundwater capture by anthropogenic groundwater extraction. There are numerous investigations of groundwater extraction capturing streamflow using methods described in Barlow and Leake (2012); however, this study takes a novel approach by looking at headwater streamflow being affected by spring diversions, which extract groundwater under gravity flow.

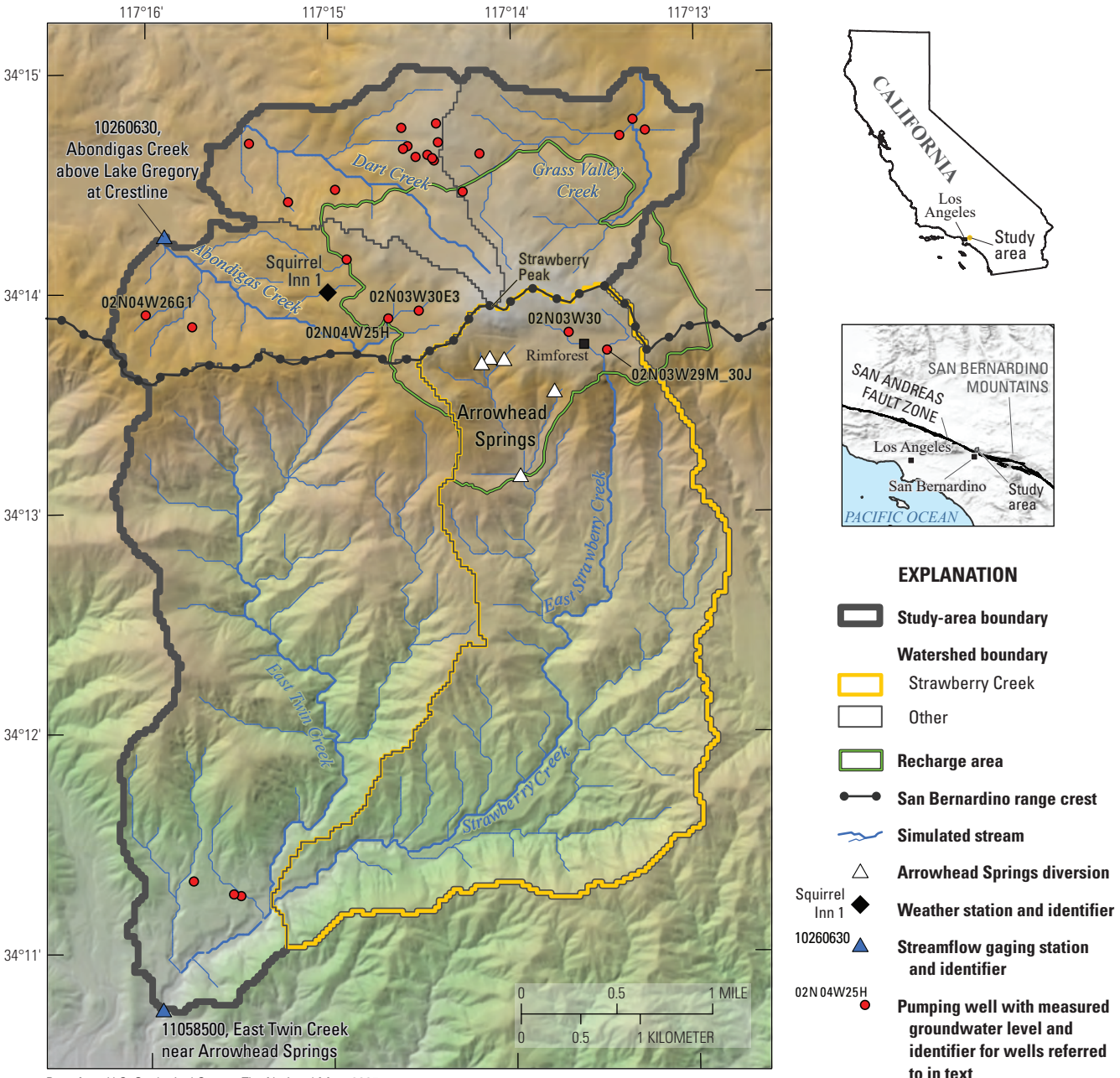
[1]U.S. Geological Survey.

[2]U.S. Geological Survey, retired.

The Strawberry Creek watershed in the San Bernardino Mountains of southern California (fig. 1) is a representative semiarid headwater watershed with spring diversions and a vulnerable stream habitat dependent on groundwater base flow. A group of natural springs referred to as the Arrowhead Springs are in the uppermost subdrainage, the upper west branch. These springs have been modified by the construction of borings and tunnels to extract groundwater under gravity and convey it through pipelines out of the watershed (Dames & Moore, Inc., 1999) Because of the typically low mean streamflow of 5.0 cubic feet per second (ft^3/s; U.S. Geological Survey, 2024) exiting the Strawberry Creek watershed, even small changes in base flow can have substantial effects on dry-season streamflow and riverine habitat. Thus, it is important to determine how these types of structures can affect headwater streams.

Strawberry Creek watershed hydrogeology is understudied, with no peer-reviewed published studies available as of 2026. The reports referenced here are consultant reports for the U.S. Forest Service and reports prepared by the National Forest Service. Information on the hydrogeological subsurface and groundwater levels is limited to 25 boreholes. Previous investigations of Arrowhead Springs include a report by Dames & Moore, Inc. (1999), which reported on the history of Arrowhead Spring diversion structures and their hydraulic connection to groundwater. The National Forest Service also published a report on the hydrogeology of the Arrowhead Springs local area describing surficial geology, faults, and stream-groundwater dynamics (Bearmar, 2017).

A study of the Arrowhead Springs and streamflow in Strawberry Creek described the stream network and streamflow and the hydraulic connection between spring diversions (Haley & Aldrich, Inc., 2022) using the Soil Water Assessment Tool (SWAT; Guzman and others, 2015) linked with the U.S. Geological Survey (USGS) modular groundwater flow model software MODFLOW (Harbaugh, 2005) to simulate the flow in Strawberry Creek. The model extent included the upper half areas of the East Twin Creek and Strawberry Creek watersheds, assuming a no-flow boundary along a groundwater divide at the San Bernardino Mountains range crest, which is the drainage divide between the northern and southern watersheds (fig. 1). The Haley & Aldrich, Inc. (2022) model had a simulation period of only 4 years, so it was not capable of analyzing long-term effects. Nonetheless, the model showed that spring diversions caused a 10-percent decrease in simulated streamflow in Strawberry Creek at a location referred to as the “confluence virtual gage,” which is located just upstream from the confluence of Strawberry Creek and east Strawberry Creek (fig. 1). Several streamflow measurements were made at this location in Haley & Aldrich, Inc. (2022), and simulated streamflow also was extracted from the current model at this location.



Base from U.S. Geological Survey, The National Map, 2025
California State Plane Coordinate System
North American Datum of 1983

Figure 1. Location of the study area, watersheds within the study area, Strawberry Creek subdrainages, Arrowhead Springs and diversion structures, municipal wells, weather station, town of Rimforest, streamflow-gaging stations, and recharge area (Morton and Miller, 2006; Bearmar, 2017; Haley & Aldrich, Inc., 2022) in San Bernardino County, California.

Study Area Description

The Strawberry Creek watershed study area is about 70 miles (mi) east of Los Angeles (fig. 1). The study area is 12 square miles and includes Arrowhead Springs in the headwaters of Strawberry Creek and the adjacent watersheds to the north (an unnamed creek referred to locally and herein as Abondigas Creek, Dart Creek, and Grass Valley Creek) and west (East Twin Creek). The study area has about 4,900 feet (ft) of physical relief, rising from about 1,200 ft above the North American Vertical Datum of 1988 (NAVD 88) at the base of the range front on the south, to about 6,100 ft above NAVD 88 at Strawberry Peak. Elevation of the Arrowhead Springs local area, located in the upper west branch subdrainage, ranges from about 4,150 to 5,330 ft above NAVD 88.

The study area climate is highly variable annually, seasonally, and with elevation. The mean annual precipitation during the period of study was 26.8 inches (in.), and total annual precipitation ranged from 8.9 in. in 1999 to 62.7 in. in 1983 (Arguez and others, 2024). The area is much cooler and wetter at higher elevations along the San Bernardino Mountains range crest compared to the base of the range front. At the Squirrel Inn 1 weather station (ID number 048476; Western Regional Climate Center, 2023) near the top of the San Bernardino Mountains (fig. 1), at an elevation of 5,250 ft above NAVD 88, mean monthly precipitation is 5.5 in. during the wet season (December through March) and 0.8 in. during the dry season (April through November). At the San Bernardino weather station, located about 3 mi south of the study area, at an elevation of 1,140 ft above NAVD 88, mean precipitation is less than half that of the Squirrel Inn 1 weather station—2.4 in. for the wet season and 0.3 in. for the dry season (Haley & Aldrich, Inc., 2022).

Precipitation falls as rain in the lower elevations, but in the higher elevations, precipitation can occur as snow. The Squirrel Inn 1 weather station has recorded a mean maximum annual snow depth of 6 in. for January through March, and a mean annual total snowfall of 37.5 in. Mean monthly temperature at the Squirrel Inn 1 weather station ranged from 32 degrees Fahrenheit (°F) in December to 67 °F in August. In San Bernardino, the mean monthly temperature ranged from 53 °F in December to 79 °F in August (Arguez and others, 2024).

Hydrogeology and Groundwater Flow

The San Bernardino Mountains are part of the Transverse Ranges and bounded on the southwest side by the San Andreas fault zone near the southern tip of the study area (Morton and Miller, 2006). Several faults and splays from the San Andreas fault zone cut across the range front. Deformation along the San Andreas fault zone and unloading of the batholith has caused fracturing of the bedrock, and weathering at the surface has created what is generally referred to as decomposed granite. Decomposed granite is unconsolidated and includes active axial channel alluvium, talus, colluvium, landslide, alluvial fan, and wash deposits. Decomposed granite is estimated at 50 ft to 180 ft thick and highly variable based on well logs. Decomposed granite is described as poorly sorted, ranging from clay and silt to cobbles.

Decomposed granite overlies faulted and fractured crystalline rock described as the San Bernardino Mountains assemblage (Morton and Miller, 2006). For this study, crystalline rocks generally are referred to as granitic bedrock. Most faults and fracture zones trend approximately east to west, as shown on figure 1. Bearmar (2017) suggests that this part of the San Bernardino Mountains appears similar to a Riedel model of right simple shear trending northwest along the San Andreas fault. Using the San Andreas fault zone as the shear zone trending about 300 degrees, the Riedel model predicts normal faults trending approximately north to south, such as L-4, and reverse faults, such as the Waterman Canyon fault strands, trending approximately east to west (fig. 1). Most faults and fracture zones are generally oriented less than 45 degrees from east to west.

Fault orientation and Riedel deformation suggests that the overall fracture fabric has more east-to-west fracture density and connectivity than north to south, which, because of fluid travel along fractures and fracture connectivity, creates an average horizontal hydraulic conductivity (HK) anisotropy (HANI), such that HK is generally much higher in the east-to-west direction than north to south.

Hydrogeology of faults typically consists of highly variable HK, with both direction and location within the fault zone (Folch and Mas-Pla, 2008; Bense and others, 2013). Characteristics of deformation are dependent on the rock mechanics and the type of stress—compression, extension, or transform—that formed the fault; however, in a general sense, HK parallel to faults and fracture zones is typically orders of magnitude higher than it is perpendicular to the fault because of limited fracture connectivity, and in many places, extremely low HK fault gouge (Mayer and others, 2007; Bense and others, 2013; Duan and others, 2017).

Faults are very common in California, and in groundwater studies, they are typically simulated as partial barriers to groundwater flow (Zhen and Martin, 2011; Siade and others, 2014). Because of high fluid and confining pressure at hundreds of feet below the surface, HK values also can be variable with depth, ranging from 5.12×10^{-18} feet per day (ft/d) for gouge (Duan and others, 2017) and 2.4×10^{-10} (Evans and others, 1997) to 7.32×10^{-12} ft/d (Wibberley and Shimamoto, 2003) for the highly fractured rock adjacent to the fault core, referred to as the "damage zone." Faults described in Bearmar (2017) have a damage zone of variable thickness, but only one fault, the Rimforest fault, has fault gouge in the core observed in the outcrop. Fault gouge may also be present in other faults, such as the splays of the Waterman Canyon fault. Thus, our study assumes that the HK of the Rimforest fault is lower than the other faults, and all fault damage zones create zones of efficient groundwater movement in the damage zone parallel to the fault.

Lineaments interpreted as faults and fracture and shear zones in the Arrowhead Springs area are shown in detail on figure 2 (Bearmar, 2017). A shear zone, L-1 has near-parallel joints that are approximately vertical. With crushed and weathered bedrock, L-2 is also a shear zone. With gouge flanked by jointed rock, L-3 is a shear zone. Finally, L-4 is a single normal fault with the east side dropped approximately 20 ft and most likely having little effect on hydraulic conductivity. The Rimforest fault is a fault zone with two parallel faults, fault gouge, and adjacent jointing that possibly has been active during the late Holocene.

Where faults and fracture zones traverse the slope and are perpendicular to the direction of groundwater flow, they restrict groundwater flow, causing the water table to rise above the land surface in stream channels and creating base flow and springs (Bearmar, 2017). The longest faults in the study area are the north and south strands of the Waterman Canyon faults (fig. 2), which are compressional reverse faults. Several faults also crisscross the study area, and in the Arrowhead Springs locale, several faults trend approximately northeast to southwest and northwest to southeast directions.

Bedrock fracture density and associated secondary HK typically decreases with depth below the land surface (Freeze and Cherry, 1979); thus, fractured bedrock is subdivided here into upper and lower hydrogeologic units. The upper fractured granite is estimated to be about 600 ft thick; however, this figure is approximate because the change in fracture density with depth is most likely gradational. It is not known or estimated how deep the fractures extend to accommodate groundwater flow, but it is assumed that groundwater flow predominantly takes place in decomposed granite and upper parts of the fractured bedrock.

There are few data on groundwater levels in the study area and none in the Arrowhead Springs locale. The pumping wells shown on figure 1 all have a single water-level measurement taken at different times. Most wells are located on the north side of the range or at the south foot, and only three wells are in the general vicinity of Arrowhead Springs—02N04W25H, 02N03W30E3, and 02N03W30 (fig. 1).

Because of recharge along the San Bernardino Mountains range crest, it is assumed to be a groundwater divide that is highest at Strawberry Peak. Groundwater generally is assumed to flow to the north and south away from the range crest and from north to south down the range front in the Strawberry Creek watershed. The fractured rock and unconsolidated surficial deposits are assumed to be unconfined throughout.

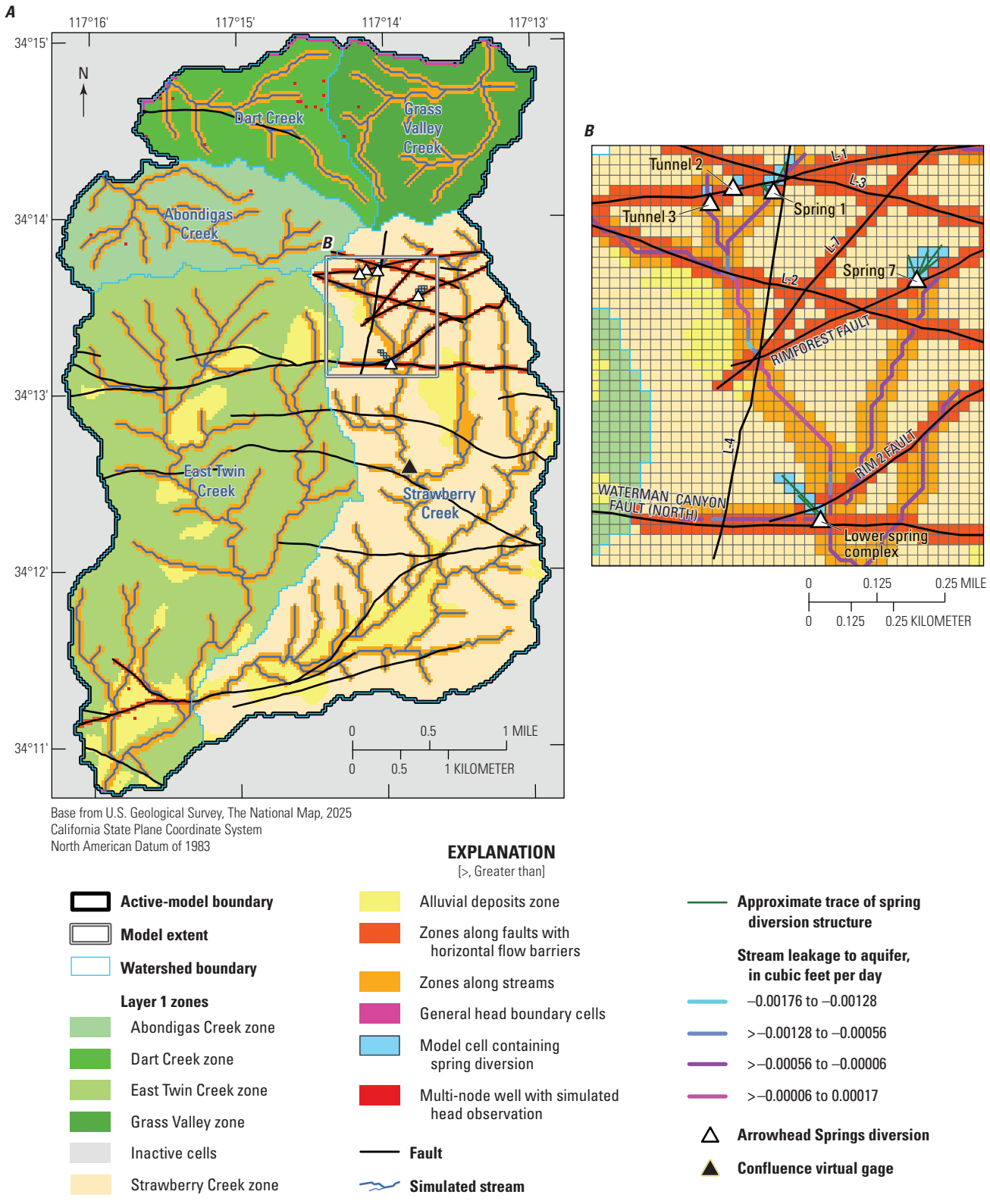


Figure 2. *A*, Strawberry Creek Integrated Hydrological Model extent, watersheds, model cells, layer 1 parameter zones, fault horizontal flow barriers, spring diversions, general head boundary cells, confluence virtual gage, and simulated streams (Ryter, 2025); and *B*, detail of local Arrowhead Springs area with simulated stream leakage to the aquifer (positive) and gain (negative) from groundwater (Ryter, 2025), San Bernardino County, California.

Sources of Recharge

Groundwater recharge is greatest in the higher elevations of the study area because of increased rain and snow that results in deep percolation. Haley & Aldrich, Inc. (2022) delineated a recharge area surrounding Arrowhead Peak (fig. 1) where most of the groundwater recharge takes place. It is interpreted that runoff to streams during snow melt and the rainy season provides groundwater recharge through soil infiltration and stream leakage, particularly in the headwaters where stream channels are above the water table for the most part. The amount of recharge in the study area has not been studied and is not quantified here as a model input but is calculated by the runoff model as part of calibration.

Mechanisms of Discharge

Groundwater discharges to streams as base flow, particularly in the lower parts of the East Twin Creek and Strawberry Creek watersheds. Some groundwater also is assumed to leave the Dart Creek and Grass Valley Creek watersheds as underflow to the north, and the East Twin Creek and Strawberry Creek watersheds to the south. The only hydrological data available to calculate a water budget for the study area are streamflow observations for the Abondigas Creek (USGS streamflow-gaging station 10260630) and East Twin Creek (USGS streamflow-gaging station 11058500) streamflow-gaging stations, reported annual spring diversion discharge, and pumping rates for water-supply wells. The largest discharge of groundwater is expected to be to evapotranspiration (ET) by vegetation and base flow to streams.

Natural Discharge

Natural groundwater discharge includes base flow to springs and streams, groundwater underflow to other watersheds, and uptake and ET by plants. The underflow to other watersheds has not been quantified but is assumed to be minimal because of groundwater divides that can form along drainage divides. Because groundwater flows away from the San Bernardino Mountains range crest, underflow is assumed to occur along the northern watershed boundaries and where East Twin Creek leaves the model area. A study by consulting firm Haley & Aldrich, Inc. (2022) estimated that more than half of precipitation is lost to plant ET either through uptake from the soil or groundwater.

Spring Diversion Structures

The Arrowhead Springs diversion structures first constructed were Tunnels 2 and 3 (fig. 2), excavated in the 1930s (Dames & Moore, Inc., 1999). Other diversions consisted of borings installed circa 1950. The diversions are plotted on figure 2*B,* with the boring traces as green lines (tunnel traces are too short to show). The diversion structures have low gradients and collection points at or near the natural springs. Diversions penetrate faults and fracture zones from the south to where head is higher. Spring diversion sites include Spring 1, Tunnel 2, Tunnel 3, Spring 7, and Springs 10, 11, and 12, which are referred to as the "Lower Spring Complex." Borings are 2-inch diameter galvanized steel pipe with screens. Spring 1 has three borings into the mountain front ranging from 121 to 197 ft long. Tunnel 2 is 26 ft long, and Tunnel 3 is 89 ft long. Spring 7 is a complex of four horizontal borings that range from 230 to 397 ft long. Springs 10 to 12 of the lower spring complex are located very close together, with three borings that are 305, 312, and 322 ft long. Tunnels were excavated into the slope and have a gravel base that allows groundwater to seep into the tunnel and be collected into pipes at the tunnel opening. Flow from tunnels and borings is piped to the bottom of the range front and removed from the hydrological system.

Since 1981, total annual flow from each spring diversion was required to be reported by companies using the water. The total mean flow reported for all spring diversions was 0.282 ft^3/s (Western-San Bernardino Watermaster, 2023). The annual flow from each spring and the total are plotted on figure 3. Reported annual flow from diversions is variable and is assumed to be affected by precipitation, which should affect groundwater recharge. There is a general correlation between total spring diversion flow and precipitation (fig. 3*F*), but there are exceptions, such as 1989, which had no reported spring diversion flow, and 2004, which had very low flow. Neither of these years were particularly dry periods, and it is highly unlikely that groundwater head dropped below the elevation of all spring diversions. Thus, the reported flow does not necessarily reflect a natural spring because diversions were not operating to capacity or were even inactive for some years.

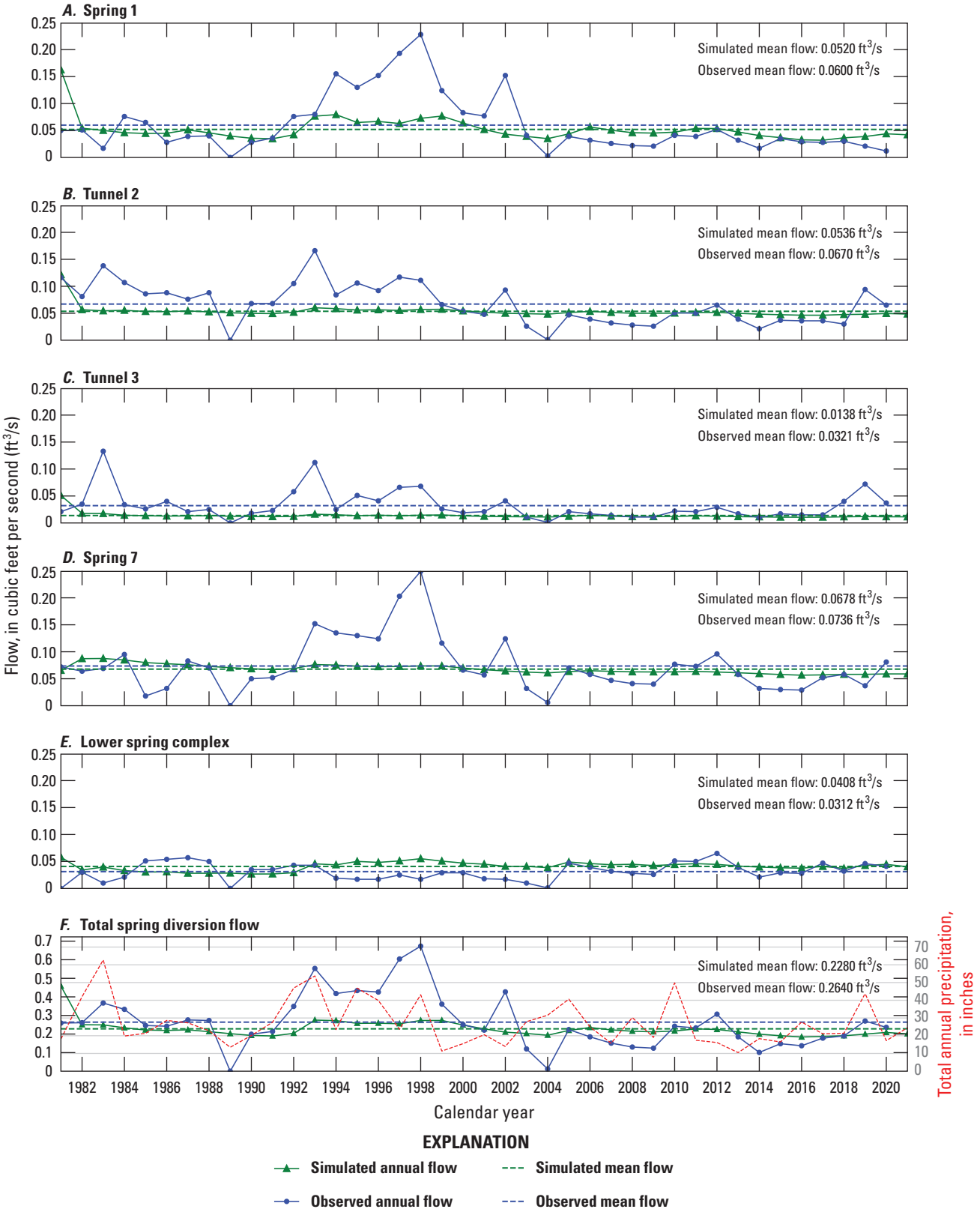


Figure 3. Simulated and measured spring diversion flow rate (Western-San Bernardino Watermaster, 2023) for individual spring diversion complexes (*A*–*E*) and the combined spring diversion flow (*F*) with total annual precipitation, Strawberry Creek Integrated Hydrological Model (Ryter, 2025), San Bernardino County, California.

Pumpage

Groundwater pumping in the study area is used for municipal and domestic purposes and irrigation of recreation areas. Most of the pumping wells are located far to the north and south of Arrowhead Springs (fig. 1) and are interpreted to have no effects on spring or streamflow. Pumping wells in the model were located from information on drillers' logs and the Crestline Village Water District (CVWD) 2020 Urban Water Management Plan (Albert A. Webb Associates, 2021). If the precise location information of wells was not available from drillers' logs, they were located within the reported township, range, and section for the well specified on the log.

Annual pumpage for the CVWD service area was reported for 2001–20 (Albert A. Webb Associates, 2021). Annual pumpage for CVWD well 2N/4W-26G1 (fig. 1) was reported separately for 1981–2013 (San Bernardino Valley Municipal Water District, written commun., November 28, 2005, August 9, 2014). Pumpage for four of the CVWD wells was estimated for 1981 to 2000 and 2021. Pumpage for 2N/4W-26G1 was estimated for 2014–21. Pumpage for domestic and irrigation purposes for 1981–2021 was estimated as described in subsequent paragraphs. Figure 4*A* shows the total annual pumpage for the simulation period.

Only 27 percent of the service area for CVWD overlies model domain; hence, 27 percent of the reported pumpage was used in the model. The reported pumpage for well 2N/4W-26G1 was subtracted from this value over the overlapping period of record (2001–13). The resulting pumpage was distributed evenly to the four wells without specified pumpage. Pumpage for 1981–2000 was estimated by 1) calculating the fraction of reported pumpage for well 2N/4W-26G1 to total pumpage in the model domain for 2001–21; 2) averaging the calculated fractions; and 3) dividing the pumpage for well 2N/4W-26G1 by the averaged fraction to estimate the total pumpage in the model domain. The pumpage for well 2N/4W-26G1 was subtracted from the total pumpage. Pumpage for 2020 was used for 2021. If reported pumpage for well 2N/4W-26G1 was zero, pumpage for the other wells was estimated from previous years.

Pumpage in the town of Rimforest area was represented by two wells near the location of well 02N03W30. Pumping data for 1981–85 were available for one of the two wells. Pumping in that well was discontinued after 1985 (San Bernardino Valley Municipal Water District, written commun., November 28, 2005, August 9, 2014). Pumpage for the other public-supply well was estimated using the average per-capita CVWD pumping rate in the model domain for 2001–10 and an estimated population of 183 for the town of Rimforest (https://places.us.com/california/rimforest/, accessed April 2024). Pumpage for public supply was discontinued, however, and it was assumed that well 02N03W29M_30J, which had been used for dewatering a landslide area near Rimforest (Haley & Aldrich, Inc., 2022), was used for municipal water supply from that point on. Pumpage was estimated for 1981–2005 when the well was abandoned (Haley & Aldrich, Inc., 2022). Pumpage in the town of Arrowhead Springs was represented by four municipal wells in the south end of the model active area. Pumpage data were available for 1998–2013 (San Bernardino Valley Municipal Water District, written commun., November 28, 2005, August 9, 2014). Pumpage for 1998 was used for 1981–97 and 2013 for 2014–21.

Domestic pumpage was estimated for 2001–21 by calculating the per capita pumping rate by dividing the total pumpage by the available population data (Albert A. Webb Associates, 2021) in the CVWD service area. Assuming four occupants per house, the resulting rate was multiplied by four. Domestic pumpage for 1981–2000 was estimated using a regression between reported total pumpage and population for the CVWD service area for 2001–20 (fig. 4*B*). The regression equation was used with population estimates for 1981–2000 to calculate pumpage. The population was estimated using an average growth rate of 0.8 percent (Albert A. Webb Associates, 2021) multiplied by the population in 2001. Pumpage per household was calculated as described previously.

Pumpage for parks and golf courses was based on average water use for turf grass of 0.2 in. per day (Kneebone and others, 1992). This value was multiplied by a representative irrigated area (about 51,505 square feet). The resulting pumpage was used for the three irrigation wells and held constant for the simulation period. Pumpage for a public supply well near the northern boundary of the model area was based on results from a yield test at the time the well was drilled.

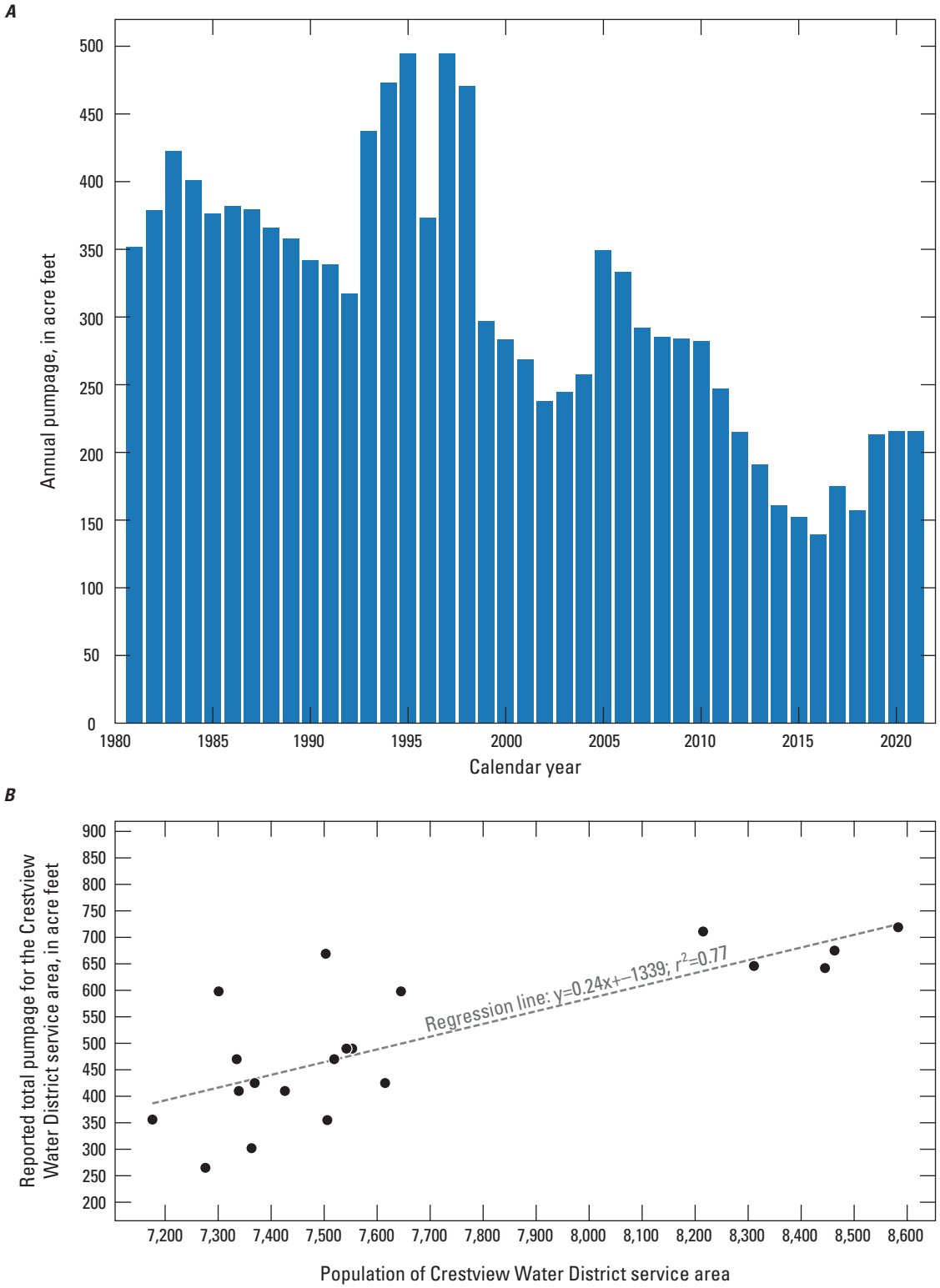


Figure 4. *A*, Total estimated annual pumpage in the Crestview Water District service area; and *B*, regression used to estimate the annual domestic pumpage in the Strawberry Creek Integrated Hydrological Model, San Bernardino County, California. Data are summarized from San Bernardino Valley Municipal Water District (written commun., November 28, 2005, August 9, 2014).

Watershed Characteristics

Near the south end of the study area, Strawberry Creek flows into East Twin Creek, which continues flowing southward out of the East Twin Creek watershed to the Santa Ana River. The southward-draining Strawberry Creek and East Twin Creek watersheds are considerably larger, steeper, and have greater relief compared to the northward-draining watersheds of Abondigas Creek, Dart Creek, and Grass Valley Creek (fig. 1).

Land cover and soils affect plant ET and water infiltration, respectively. Land cover for the East Twin Creek and Strawberry Creek watersheds is mostly mixed chaparral land (fig. 5). *Pinus jeffreyi* Balf. (Jeffrey pine) is prevalent at the higher elevations, which receives more precipitation. The pines have deep roots that provide access to groundwater and increase ET. Local areas of montane hardwood occur in all watersheds. The northern watersheds have a higher percentage of urban land cover, and the southern watersheds consist mostly of natural land cover because of the steep terrain. Land cover in the vicinity of Arrowhead Springs is more variable and includes barren land as well as urban land cover upstream from the springs and montane hardwood downstream from the springs.

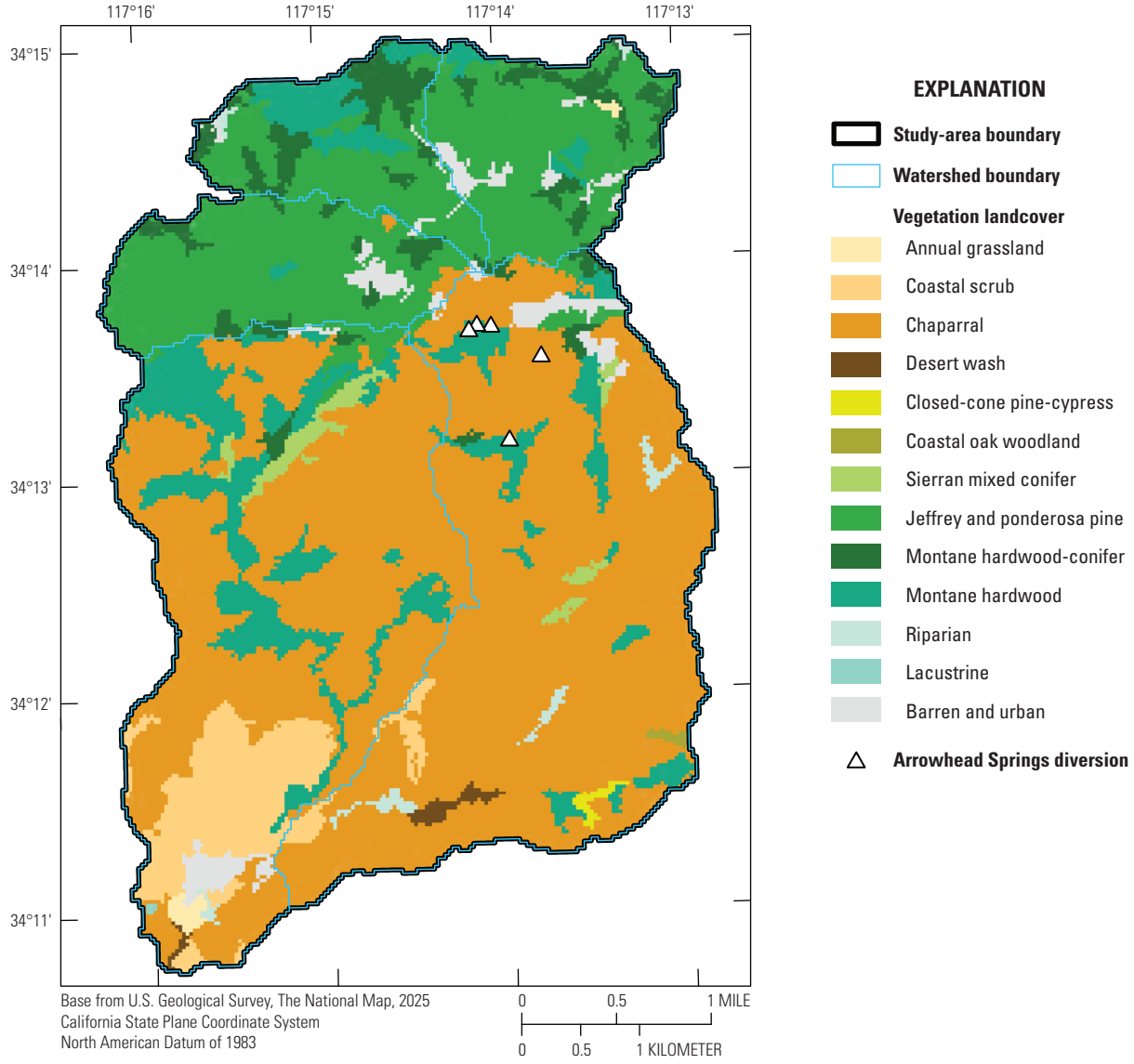


Figure 5. Land cover with vegetation types for the Strawberry Creek study area (California Department of Forestry and Fire Protection, 2023), San Bernardino County, California.

Land cover for the three northward-facing watersheds is primarily forested, dominated by Jeffrey pine (California Department of Forestry and Fire Protection, 2023), as compared to the south-facing watersheds that have mostly mixed chaparral land cover (fig. 5). Jeffrey pine is prevalent at the higher elevations, which receive more precipitation. The pines have deep roots that provide access to groundwater and increase plant ET. Local areas of montane hardwood occur in all watersheds. The northern watersheds have a higher percentage of urban land cover. Although not represented by the land cover map, the northern watersheds contain a higher percentage of developed land in terms of rural residential lots within the forested land cover, and these developed lands include roads and some local areas of denser development, such as commercial land uses. In contrast, the southern watersheds consist mostly of natural land cover because of the steep terrain. Land cover in the vicinity of the springs is more variable and includes barren land as well as urban land cover upstream from the springs and montane hardwood downstream from the springs.

Values of the root zone storage capacity range from 5 to 34 in., with a mean value of 12 in. for the study area (U.S. Department of Agriculture, 2003). The upper root zone storage parameter, used to represent the part of the root zone where both transpiration and evaporation occur, was estimated as a function of the capacity, and ranged from 5.5 to 24 in., with a mean value of about 8 in. for the study area.

Soil properties also vary between the northern and southern watersheds. The northern three watersheds are almost entirely coarse-loamy soils, whereas the southern two watersheds contain mostly sandy-skeletal soils in the headwater areas and loamy soils in the lower drainages (U.S. Department of Agriculture, 2003). Coarse-loamy soils occur directly upstream from Arrowhead Springs along the San Bernardino Mountains range crest. Areas of fine-loamy soil occur downstream from the springs, mostly within the Strawberry Creek watershed. Sandy skeletal soil is the dominant soil type in the upper west branch Strawberry Creek subdrainage and is the soil texture type occurring at the location of all the Arrowhead Springs.

Streamflow

Streamflow in the study area is highly variable and episodic (flashy), with peak flows having short response times to storm events (U.S. Geological Survey, 2024). Overland flow contribution to streamflow tends to be rapid and short because of the prevalence of steep slopes and thin soils formed on discontinuous decomposed granite and fractured granite. During winter and early spring months, some runoff occurs in response to snowmelt and tends to be less episodic, resulting in longer periods of streamflow above base flow conditions.

The USGS East Twin Creek streamflow-gaging station 11058500 has a period of record from December 27, 1919, through the period of analysis, 1981–2021. Mean streamflow for the period of record through 2021 was 5.0 ft^3/s, and the maximum daily flow was 795.0 ft^3/s on February 25, 1969 (U.S. Geological Survey, 2024). The month with the greatest mean monthly streamflow was March (12.1 ft^3/s) and the month with the lowest mean monthly streamflow (1.1 ft^3/s) was September.

The Abondigas Creek streamflow-gaging station (fig. 1) has a period of record from March 8, 1979, to September 30, 1993 (U.S. Geological Survey, 2024). Mean streamflow for the period of record was 42.4 ft^3/s, and the maximum daily flow was 103.1 ft^3/s on January 29, 1980. Streamflow at this gage is intermittent, with no measured streamflow for about 29 percent of the period of record. March had the greatest mean monthly streamflow (4.2 ft^3/s), and August had the lowest mean monthly streamflow of 0.07 ft^3/s.

Base flow to streams in the East Twin Creek and Strawberry Creek watersheds was estimated using base-flow separation performed on streamflow measurements collected at the East Twin Creek streamflow-gaging station (U.S. Geological Survey, 2024) using the hydrograph-separation program, HYSEP (Sloto and Crouse, 1996). For the period of record, calculated base flow occurred just after wet months and peaked in March, whereas total streamflow peaked in February (fig. 6). The mean annual proportion of the total streamflow made up of base flow, referred to as the base-flow index (BFI), was 0.70. The monthly BFI showed that during the wet months of October through April, mean streamflow was 5.0 ft^3/s, runoff was dominant, and BFI was lower. During dry months, mean streamflow was 2.1 ft^3/s, and the BFI was 0.95. High mean annual BFI shows how streamflow is very dependent on base flow for a good part of the year. Base-flow separation also was performed on the Abondigas Creek streamflow-gaging station on the north side of the range (fig. 1), finding that it received less base flow and had a mean BFI of 0.40.

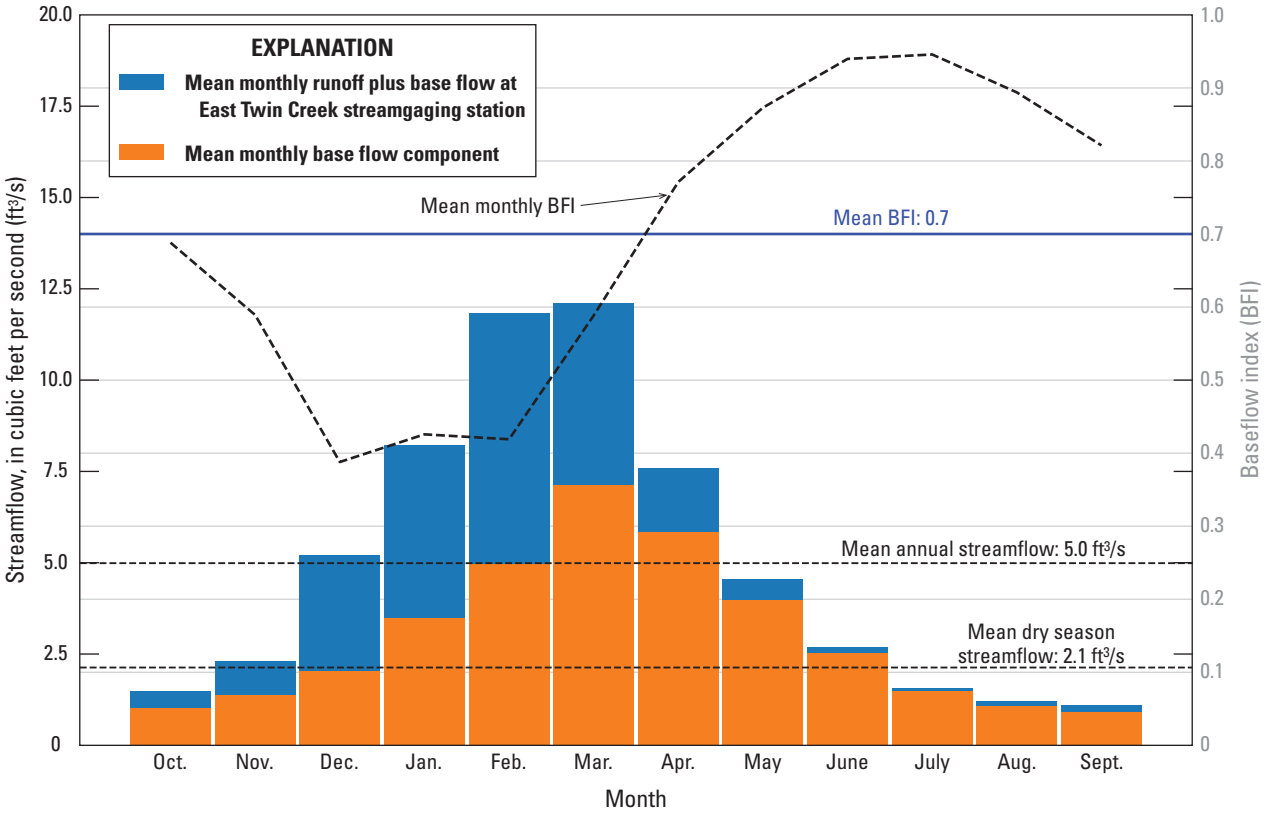


Figure 6. Mean monthly streamflow measured at the East Twin Creek streamflow-gaging station near Arrowhead Springs, streamflow-gaging station 11058500 (U.S. Geological Survey, 2024), period of record 1981–2021, and base flow calculated using the HYSEP hydrograph-separation method of Sloto and Crouse (1996), with the base-flow index (BFI; base flow/streamflow), San Bernardino County, California.

Strawberry Creek Integrated Hydrological Model

The Strawberry Creek Integrated Hydrological Model (SCIHM) was developed using GSFLOW, the U.S. Geological Survey (USGS) Groundwater and Surface-water Flow model (Markstrom and others, 2008). Coupled with the modular groundwater-flow model, MODFLOW (Harbaugh, 2005), GSFLOW is a surface runoff model, Precipitation-Runoff Model System (PRMS; Markstrom and others, 2015). The SCIHM active area includes the Strawberry Creek, East Twin Creek, a stream locally referred to as Abondigas Creek, Dart Creek, and Grass Valley Creek subbasins (fig. 1).

Boundaries and Model Discretization

Spatial discretization is 3 layers of 263 rows and 176 columns of cells, 100 ft on a side. The land surface is the top of the model. Temporal discretization is 41 annual stress periods for 1981–2021 and daily time steps for each stress period. Lateral model groundwater boundaries are based on topographically-defined drainage basins and the surface water drainage divides and were assumed also to be groundwater divides and thus no-flow boundaries. The area of focus for this study is the Arrowhead Springs area on figure 1, which is far enough from lateral boundaries to minimize boundary effects on local groundwater flow. Underflow along the northern and southern edges of the model was simulated with the General Head Boundary package (Harbaugh, 2005) shown with pink cells on figure 2*A*. It was assumed that on the south end of the model underflow only takes place where East Twin Creek flows out of the model. Pumping wells were simulated using the Well package (Harbaugh, 2005). Well-construction information from drillers' logs was used to assign wells to layers. If data were not available for a well, construction was based on reported well-construction information for a nearby well.

Streams simulated in the SCIHM are shown on figure 2*A* and were simulated using the Streamflow Routing (SFR) package (Niswonger and Prudic, 2005), which simulates streamflow and flow between streams and groundwater or the unsaturated zone. The SFR package produces a detailed budget of streamflow and loss or gain.

Simulating Spring Diversion Structures

Because the spring diversion structures function as drains, extracting water under gravity and driven by the local groundwater head, a boundary condition in MODFLOW needed to be configured. MODFLOW includes the drain package (Harbaugh, 2005) but this is not available with GSFLOW. MODFLOW also includes the Multi-Node Well package (Konikow and others, 2009), which allows horizontal wells, but they do not allow flow under gravity. Instead, the SFR package was used to extract groundwater similar to base flow. SFR also allows the length and elevation of drains to be placed in a model cell with the width and conductivity specified. Spring diversion stream segments were placed in blue cells on figure 2*B*. Flow into each stream segment was not routed to other stream segments so it leaves the model and does not return to the groundwater system as stream loss. Flow to the stream segments representing spring diversions was dependent on the head and HK of the model cell. To estimate spring diversion flow, the SFR budget file records flow between streams and groundwater and was used to determine GSFLOW calibration of spring diversion flow, and all simulated streams.

Horizontal Flow Barriers

Faults and fracture zones were simulated using the Horizontal Flow Barrier (HFB) package (Harbaugh, 2005), which allows the conductance between cells within a layer to be adjusted to simulate a vertical barrier to horizontal flow. The conductance of an HFB was set by the hydraulic characteristic (HYDCHR), which is the HK of the barrier divided by the width of the cell. All fault HFBs in a layer were assigned the same HYDCHR for the watershed where they are located, except fault L3 (fig. 2*B*), which was divided into two zones representing the east and west sections.

Precipitation-Runoff Model System

The PRMS model uses hydrological response units (HRUs) that are typically subdrainage areas with the same soil, vegetation, and other parameters. MODFLOW uses a grid with cells that are much smaller. To accommodate the variability of parameters in MODFLOW cells, each MODFLOW cell was defined as one HRU. This configuration has several advantages, including providing a simpler and more direct coupling of the PRMS and MODFLOW components and enabling a better representation of spatial variability in climate and watershed characteristics, an important consideration given the high local relief and rugged terrain of the study area. For example, local-scale variations in slope and aspect can strongly affect potential evapotranspiration (PET) simulated by PRMS. The grid-based layout also improves routing interflow and runoff downslope to stream channels.

Used as input for the PRMS model consisting of daily precipitation and maximum and minimum daily air temperature, daily climate records were collected from a network of 50 monitoring sites, as shown on figure 7 (California Irrigation Management Information System, 2023); these sites are in and surrounding the study area and helped to develop the historical climate input for the simulation period. The data were spatially interpolated to the centroid location of the study area, providing a single virtual station. Spatial interpolation was done using a modified inverse-distance squared method, where the inverse-distance-squared weighting factors were adjusted using downscaled Parameter-elevation Regressions on Independent Slopes Model (PRISM) grids (PRISM Climate Group, 2020) for 30-year mean monthly precipitation and maximum and minimum air temperature defined for calendar years 1991–2020 (Daly and others, 2008; Hevesi and Johnson, 2016). To account for orographic effects on both precipitation and air temperature throughout the study area, daily climate was spatially interpolated at all HRU locations. The mean monthly precipitation and mean monthly maximum and minimum air temperature then were calculated using the interpolation results.

The mean monthly results were used to define the monthly PRMS adjustment factors assigned to each HRU for precipitation and maximum and minimum air temperature to spatially interpolate the climate inputs to HRUs. The resulting average annual precipitation and snow for the historical period are shown for the study area on figure 8.

Critical parameters that were estimated and modified during PRMS calibration included monthly parameters used to simulate PET, parameters defining the root zone storage capacity, and parameters controlling groundwater recharge (percolation below the base of the root zone). The root-zone field capacity parameter for simulating transpiration was estimated using land cover, slope, and percentage forest canopy cover.

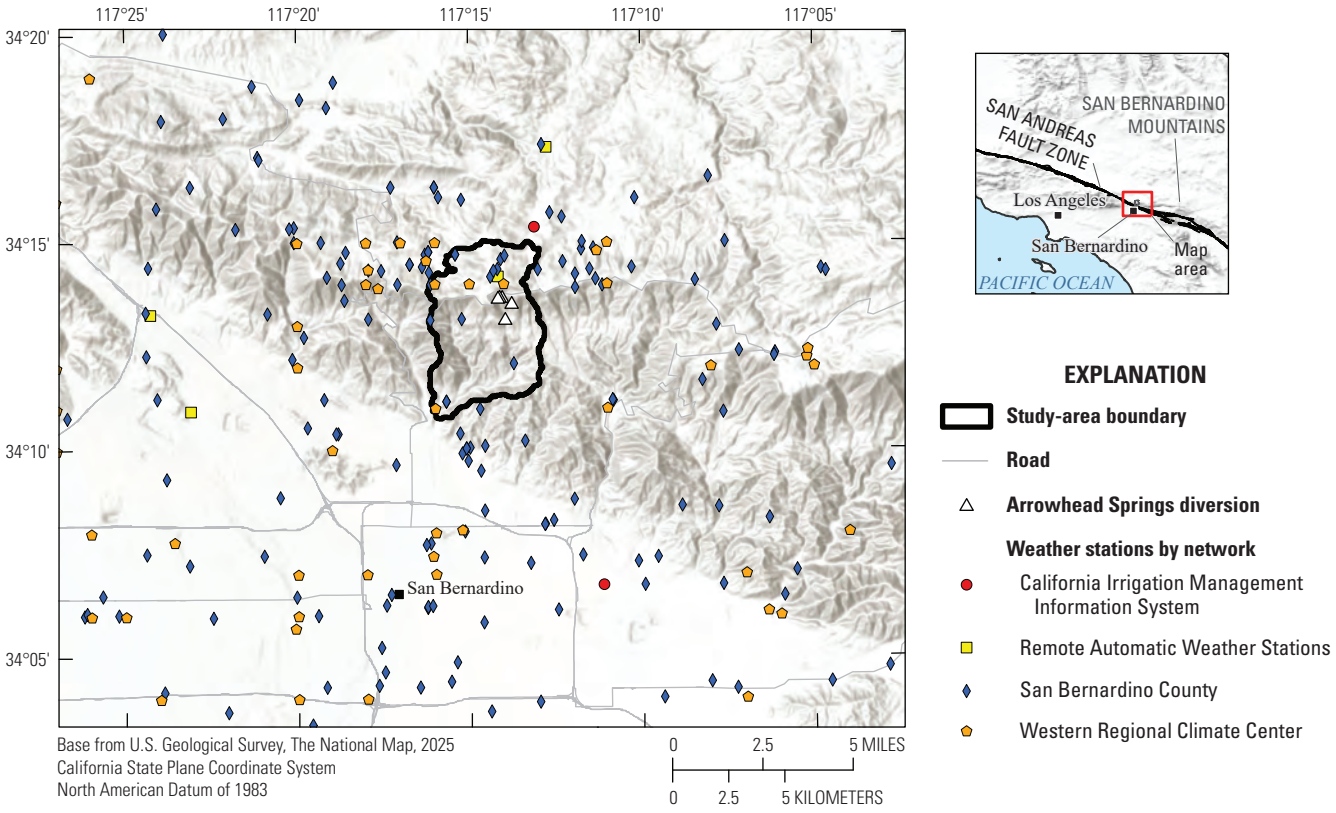


Figure 7. Locations of weather stations managed by the California Irrigation Management Information System, Remote Automatic Weather Stations, San Bernardino County, and the Western Regional Climate Center (California Irrigation Management Information System, 2023), used to calculate precipitation and temperature for climate input data for the Strawberry Creek Integrated Hydrological Model, San Bernardino County, California.

MODFLOW Model

The groundwater-flow system was simulated in GSFLOW using the Raphson-Newton formulation of MODFLOW (Niswonger and others, 2011). The groundwater model has three layers that represent materials documented in the study area and characteristics of fractured rocks in fault zones described in the "Hydrogeology and Groundwater Flow" section. Layer 1 is composed of decomposed granite, and layers 2 and 3 are the upper and lower fractured bedrock zones, respectively. It was assumed that most groundwater flow takes place in the top two layers; however, layer 1 can be dry in many places in the uplands. Because there are few locations with measured thickness of the decomposed granite, and no direct measurements of the gradational change from the upper to lower fractured zones, layer thicknesses are very approximate. The top of layer 1 is the land surface. The thickness of the decomposed granite was set at 50 ft across the model, except for the general Arrowhead Springs area, where the thickness was increased to as much as 500 ft, in essence combining the upper two layers. This combination prevented the upper layer from drying out along streams where spring diversions are being simulated, which would have caused MODFLOW to convert layers containing diversions to confined layers. In the springs area, the properties for layer 1 are representative of fractured bedrock in layer 2. The large thickness of layer 1 was also necessary where the land surface drops steeply to the south to maintain connection between cells. Model layer 2 is the upper fractured bedrock zone with a thickness of 500 ft, and layer 3 is 984 ft thick.

Decomposed granite and unconsolidated deposits are a mix of clay, silt, sand, and gravel, and HK was estimated to range from 0.1 to 10.0 ft/d (Davis, 1969). Fractured granitic rocks were estimated to have variable and horizontally anisotropic HK. Depending on fracture density and aperture, fractured igneous rock HK can range from 0.03 to 292 ft/d (Freeze and Cherry, 1979). In the study area, HK was assumed to be much lower and no greater than about 16 ft/d.

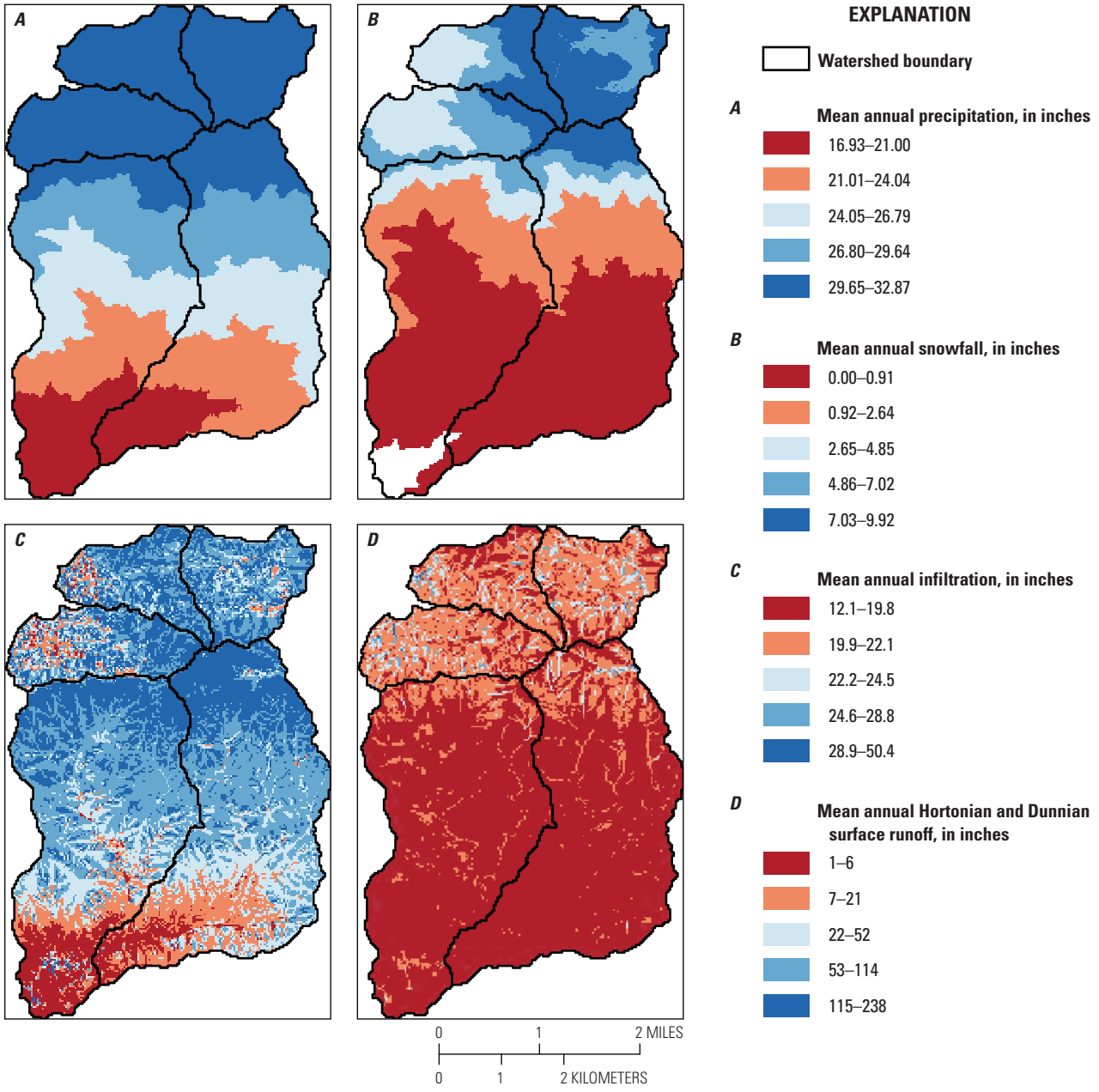


Figure 8. Mean annual *A*, interpolated precipitation; *B*, snowfall (California Irrigation Management Information System, 2023); *C*, precipitation and runoff model system (Markstrom and others, 2008) simulated infiltration; and *D*, Hortonian and Dunnian surface runoff (Ryter, 2025) for the Strawberry Creek and adjacent watersheds, Strawberry Creek Integrated Hydrological Model, San Bernardino County, California.

The fracture fabric described in the "Hydrogeology and Groundwater Flow" section results in a groundwater system that has a much higher HK in the east to west direction than north to south. The hydrogeology of faults in the Arrowhead Springs area was based on field observations in Bearmar (2017) and the conceptual model of the locations of natural springs and spring diversions. There have been no studies of the faults in the subsurface or the drop in hydraulic head across them. Fault gouge in fault cores has been observed in outcrops of the Rimforest fault, but most faults were described as fault damage zones or fracture zones.

Several assumptions were made herein to simulate the hydrogeology of faults. First, it was assumed that because of fracture connectivity in the fault damage zones and limited connectivity across the fault, the HK was much higher along the fault than across it. This simulation used an HK for a fault trending approximately east to west that was higher and a very low HANI, resulting in a much lower HK along columns. Because of gouge and the orientation of faults and adjacent fractures in the fault damage zone, HK across faults was expected to be very low, with fault gouge similar to indurated clay (Bearmar, 2017), which has a range of 3.28×10^{-11} to 3.28×10^{-8} ft/d (Davis, 1969). Low HK values in the north–south direction and along columns were simulated by using a very low HANI and simulated the fault as an HFB. For faults oriented north, HANI was close to 1 because most groundwater flow was assumed to be toward the south and parallel to the fault.

HFBs provide a resistance to flow between cells that is more effective than HANI because it can affect flow in any orientation. HFBs are simulated in MODFLOW as reduced conductance between horizontally adjacent cells. Conductance across an HFB is referred to as the hydraulic characteristic, which is the HK of the barrier divided by the thickness, in per-day units. For faults outside of the Arrowhead Springs area, a HYDCHR of 0.0001 per day was used. In the springs area, HFBs simulated fracture zones and faults with gouge, and HYDCHR ranged from 1×10^{-12} to 1.5 per day.

Away from faults, there was estimated to be more variability in fracture orientation and connectivity in multiple directions; however, the dominant fracture direction was estimated to be east to west. HANI here was estimated to range from 0.1 to 0.0001 for layers 2 and 3. Vertical hydraulic conductivity (VK) was estimated to be similar to HK in sandy and alluvial deposits, so the vertical anisotropy (VK/HK) was estimated to be 0.5, and in fractured bedrock, vertical fractures were expected to cause VK to be similar to alluvial deposits.

Parameter Zones

Hydraulic parameters were assigned to model cells using zones. All parameters for conductivity and storage were assigned to the same zones. Zones for layer one are shown on figure 2. To define zones in layer 1, each watershed was assigned a zone representing decomposed granite, with smaller zones representing unconsolidated surficial deposits, cells along streams, and cells along faults. In the Arrowhead Springs area where layer 1 is much thicker, all zones represent fractured bedrock. Each fault HFB was assigned a zone for each fault, watershed, and layer. Layer 2 and 3 zones consist of fractured bedrock and faults.

Model Calibration

Because the SCIHM integrates the soil, unsaturated, and groundwater zones, model calibration was performed in three steps, which are described in the following sections:

1. Calibration of PET, which regulates actual plant ET in the PRMS simulation;
2. Runoff, infiltration, and streamflow calibration of the PRMS simulation; and
3. Groundwater flow system calibration, primarily using flow discharge from spring diversion structures.

PRMS Calibration

Calibration of the PRMS model was done in two stages. The first stage consisted of fitting simulated and measured PET because it strongly affects actual ET, which is one of the largest model outflows. The second stage entailed fitting simulated to measured streamflow as closely as possible. Measured PET was acquired for the Lake Arrowhead station (number 192) of the California Irrigation Management Information System (CIMIS) close to the northern boundary of the study area (California Irrigation Management Information System, 2023). The published CIMIS statewide map of PET zones and the corresponding table of mean monthly PET values was also used in conjunction with the CIMIS station data for the PET calibration. In PRMS, the Jensen-Haise coefficient (jh_coef) is used in the Jensen-Haise formula (Jensen and Haise, 1963) to simulate PET. The PRMS model was run decoupled from GSFLOW, and jh_coef was manually adjusted to get the best match between simulated and measured PET. The simulated PET matched the measured PET reasonably closely (fig. 9). The mean monthly PET measured at the Lake Arrowhead climate station and simulated at the northeastern-most model cell is plotted on figure 9. The simulated PET is slightly higher than the measured PET, and the mean PET was 0.181 in., or about 21 percent higher than the mean measured PET of 0.148 in.

Streamflow records at the two USGS streamflow-gaging stations were used for the second stage of calibration. Initial calibration to streamflow was done using de-coupled PRMS simulations for a 21-year calibration period of water years 1982–2002 for the East Twin Creek and a 12-year calibration of water years 1982–93 for the Abondigas Creek calibration.

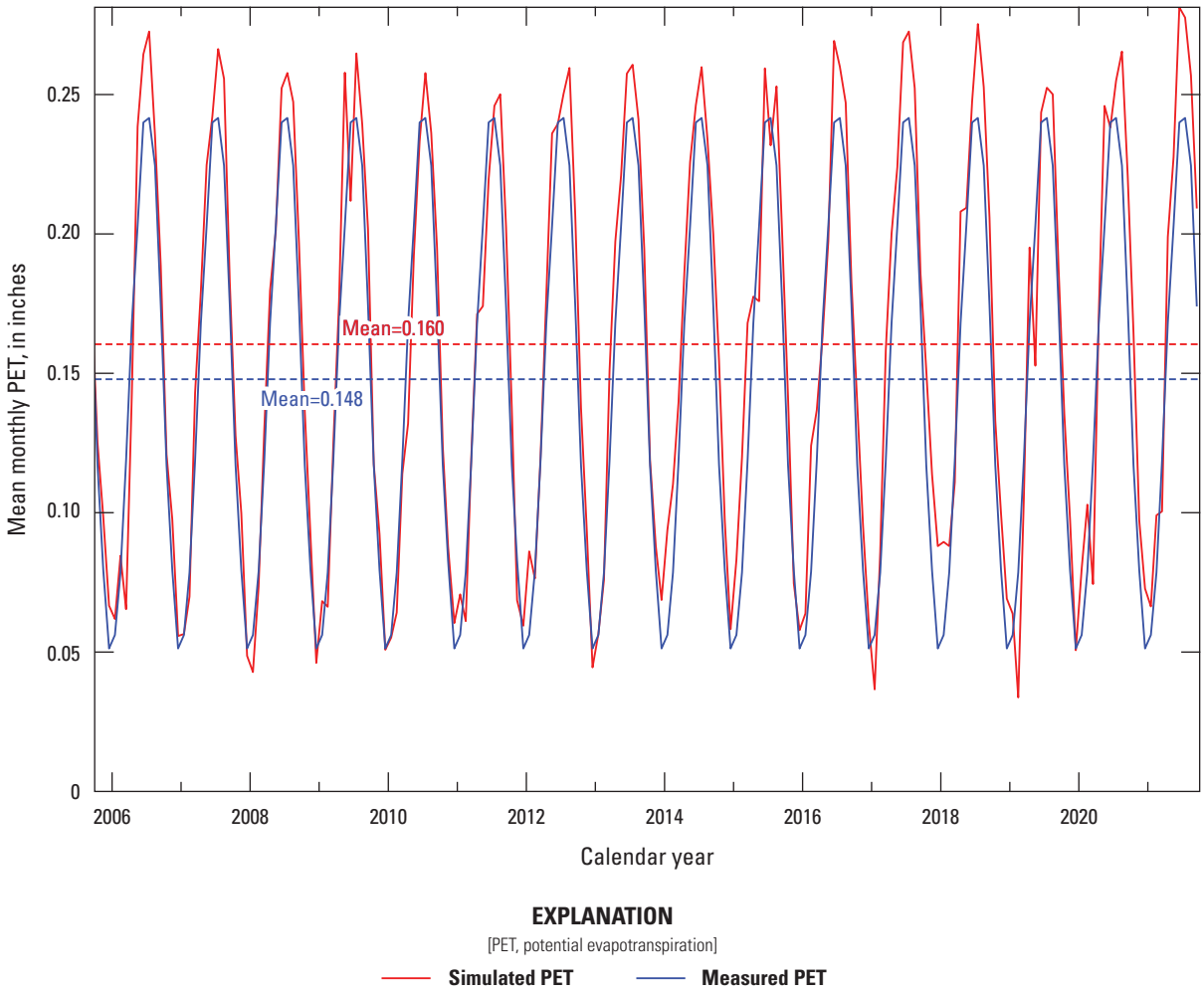


Figure 9. Simulated (Ryter, 2025) and measured (California Irrigation Management Information System, 2023) monthly mean potential evapotranspiration for the Lake Arrowhead climate station and the nearest model cell, Strawberry Creek Integrated Hydrological Model, San Bernardino County, California.

Graphical and statistical comparison between simulated and measured streamflow at the two streamflow-gaging stations indicated a satisfactory calibration. Because of the erratic, flashy nature of streamflow in the study area, the measured monthly mean streamflow values were used. The Nash-Sutcliffe efficiency (NSE) coefficient (Nash and Sutcliffe, 1970), which is 1 minus the error variance of the modeled time series divided by the variance of the observed time series, was used as a calibration statistic. The best model fit is where the NSE coefficient is equal to 1.0. For the East Twin Creek streamflow-gaging station, calibration period simulated mean streamflow qualitatively matched the observed mean streamflow (fig. 10*A*), and the mean simulated streamflow of 3.9 ft^3/s was 63 percent of the mean measured streamflow of 6.2 ft^3/s. The highest flow runoff events appeared to be most accurately simulated; however, simulated lower flow values generally were underestimated. Smaller runoff events were notably underpredicted, but the lower flow values in these events closely matched the observed flow values. The NSE was 0.60, showing that the decrease in simulated flow for lower runoff events affected the model calibration.

Simulated mean streamflow at the Abondigas Creek streamflow-gaging station generally matched measured streamflow graphically (fig. 10*B*), but the mean simulated streamflow of 0.60 ft^3/s was only 55 percent of the measured flow of 1.1 ft^3/s. The simulated flow was also positive during periods when there was no flow. This finding suggests that, in the Abondigas Creek watershed, the model overestimated base flow. Calibration statistics for Abondigas Creek were better than East Twin Creek, with an NSE of 0.77.

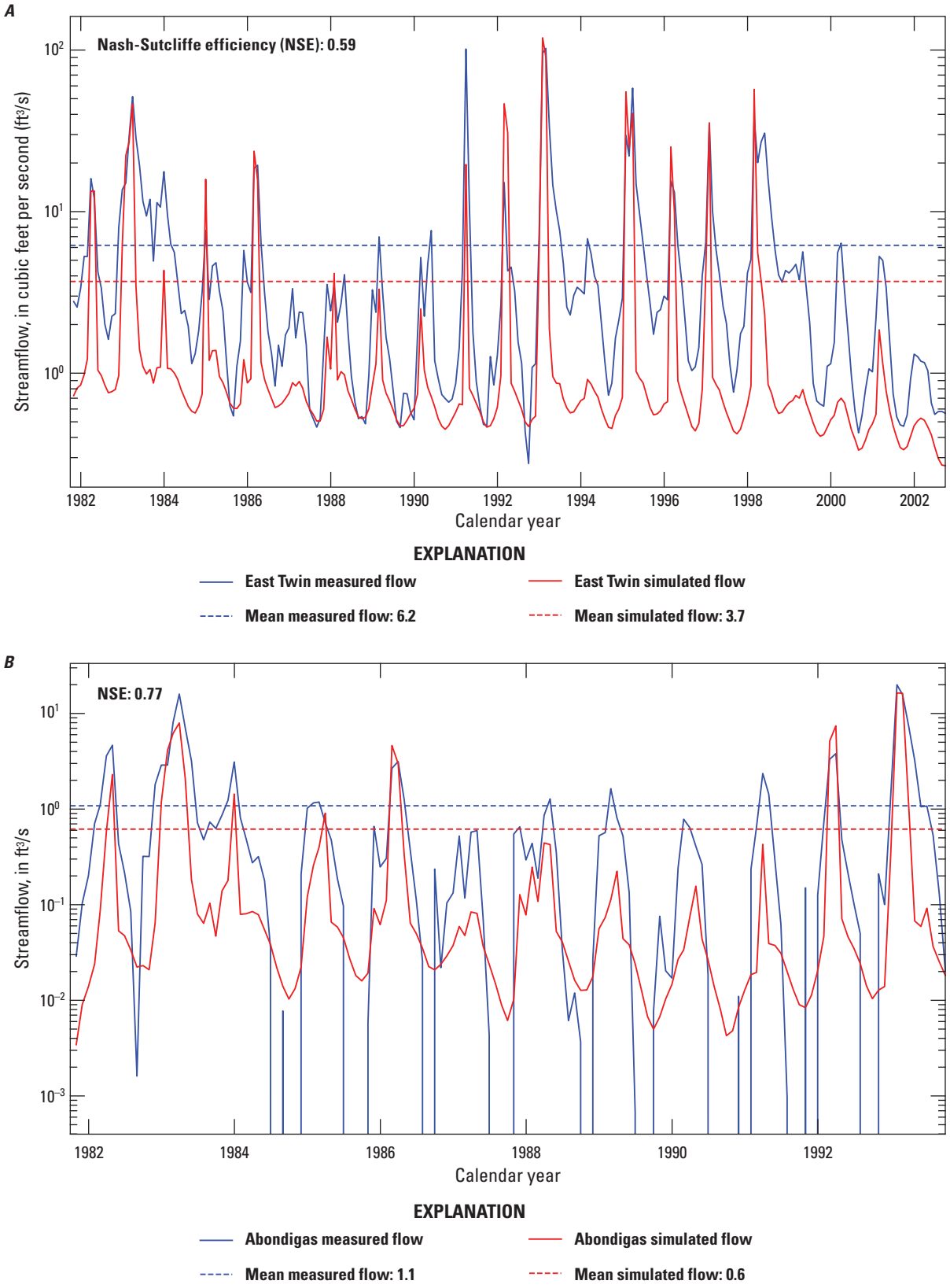


Figure 10. Simulated (Ryter, 2025) and measured (U.S. Geological Survey, 2024) monthly streamflow used for model calibration with Nash-Sutcliffe efficiency (NSE) coefficient (Nash and Sutcliffe, 1970), for *A*, East Twin Creek near Arrowhead Springs, U.S. Geological Survey (USGS) streamflow-gaging station 11058500; and *B*, Abondigas Creek at Crestline, USGS streamflow-gaging station 10260630, Strawberry Creek Integrated Hydrological Model, San Bernardino County, California. Both plots are semi-log scale.

Simulation results using the calibrated PRMS model component for historical climate included combined Hortonian and Dunnian surface runoff and land-surface infiltration that can become groundwater recharge (figs. 8*C*, 8*D*). The greatest amount of runoff and infiltration are at the higher elevations in the recharge area, delineated on figure 1, where precipitation and snowfall are also highest (figs. 8*A*, 8*B*, respectively). The mean annual simulated surface runoff using PRMS was 6.0 inches per year (in/yr) for the SCIHM area, ranging from less than 1 to 238 in/yr. Subdrainages with the highest surface runoff rates were generally correlated to the subdrainages with highest precipitation rates. Runoff for the northern watersheds was enhanced by a higher percentage of impervious areas associated with urban and developed land cover.

As with surface runoff, the subdrainages and HRUs with the highest elevation headwaters and the highest precipitation rates tended to have the highest recharge rates of 8.7 in/yr and higher. The headwater area containing Arrowhead Springs and locations in the proximity of the springs had the greatest concentration of HRUs with high recharge. For the higher elevations of the Strawberry Creek watershed, average recharge of 8.1 in/yr was 26 percent of precipitation. In comparison, basin-wide average recharge for the area of the SCIHM (4.3 in/yr) was about 16 percent of precipitation.

The summary annual statistics for the largest components of the PRMS budget are listed in table 1. The minimum and maximum values showed substantial variation year to year. Precipitation varied by almost an order of magnitude from 6.138 in. to approximately 63 in/yr. Snow also varied, ranging from 0.389 to 13.797 in/yr. Actual ET varied from 8.071 to 34.119 in/yr, and during dry years, was greater than precipitation, requiring substantial uptake from groundwater. ET was also high during dry years, which caused groundwater recharge to be very sensitive to decreases in precipitation. For the driest year in the simulation period, there was virtually no recharge, as only 0.003 in., or 0.047 percent of precipitation became recharge. Alternatively, during the wettest year, over 20 percent of precipitation became recharge. The mean proportion of precipitation that became groundwater recharge was 13.489 percent.

GSFLOW Calibration

Calibration of the MODFLOW model of GSFLOW using the calibrated PRMS model is the third stage of calibration. Because the only groundwater-head and streamflow measurements were located several miles from the Arrowhead Springs (fig. 1), MODFLOW calibration was based primarily on the reported spring diversion discharge for each spring and the reported total for all springs. The flow from springs is dependent on the groundwater head at each diversion and the hydraulic conductivity of the aquifer and the conductivity of horizontal flow barriers along the local faults that caused the groundwater head to be higher at the diversion.

As discussed in the "Spring Diversion Structures" section, the quality of reported spring diversion flow is not an exact measurement of natural flow under gravity. There are questions about years with no reported flow (1989 and 2004) and those that did not change with precipitation as expected, such as 2012 on figure 3*F*. Therefore, it was not possible to match annual flow by adjusting hydraulic parameters in the model. Instead, the model calibration goal was to match the long-term (1981–2021) mean flow from springs, which provided a simulation of the amount of water taken from the groundwater system over this period, as a function of recharge and hydraulic properties. Groundwater-level measurements also were compared to the simulated heads, and the error was calculated. SCIHM GSFLOW calibration was accomplished by manually adjusting MODFLOW parameters, primarily in the area shown on figure 2*B* and by running the GSFLOW model with the calibrated PRMS model parameters.

Table 1. Ranges and mean annual area-averaged flow in inches for the entire Strawberry Creek Integrated Hydrological Model active area (Ryter, 2025), San Bernardino County, California.

Category	Summary statistics of simulated area-averaged annual flow in inches		
	Minimum	Mean	Maximum
Precipitation	6.138	26.806	62.743
Snow melt	0.389	4.650	13.797
Actual evapotranspiration	8.071	18.867	34.119
Hortonian surface runoff	0.017	0.806	4.433
Streamflow out	0.087	7.976	42.255
Groundwater recharge	0.003	4.243	15.547
Percent of precipitation to groundwater recharge	0.047	13.489	20.312

Calibrated Parameter Values

The calibrated hydraulic parameters with the highest spring diversion flow sensitivity that were adjusted for calibration were HK, HANI, HFB, HYDCHR, and specific yield (SY), which are plotted on figure 11 for zones in layer 1. In layer 1, HK did not vary greatly, ranging from 1 to 5 ft/d (fig. 11*A*). The lowest values were assigned to the watersheds to the north and East Twin Creek, and fault parameter zones in the Strawberry Creek watershed (fig. 11*A*). For the Strawberry Creek watershed and decomposed granite, stream deposit HK values ranged from 2.1 to 3.1, and unconsolidated deposits ranged from 1.75 to 2.10 ft/d.

The HK values were affected by HANI (fig. 11*B*), which was adjusted for fault zones in the Arrowhead Springs local area to restrict flow to the south and increase flow in the east–west direction. Fault zone HANI was 0.0001–0.0010, which varied in part based on descriptions (Bearmar, 2017) and orientation (if the fault trace was not east–west along model cell rows, the anisotropy was a lower value). Because of the increased thickness of layer 1 in the area surrounding the spring diversions, decomposed granite was assigned a higher HANI, but it was still relatively low because it included fractured granite (0.0010–0.0100), and unconsolidated and stream deposits had higher values (0.0100–1.0000). As for HFB HYDCHR (fig. 11*C*) values, they were typically very low but had variable values in the Arrowhead Springs area, including faults with gouge and fracture zones without gouge (1×10^{-11}–0.0001). In terms of SY, it was assumed to be low, 0.10 in fractured bedrock (fig. 11*D*) and higher in stream axial deposits and alluvium (0.15–0.20). Vertical hydraulic conductivity was used as anisotropy (VKA). For unconsolidated deposits, VKA was equal to 1; for stream deposits, VKA was equal to 0.75; and for fractured bedrock, VKA was equal to 0.01.

Parameter zones for layers 2 and 3 for hydraulic parameters are shown on figure 12 with calibrated hydraulic parameters. Because layer 1 was thickened in the Arrowhead Springs area, spring diversion flow was not very sensitive to the lower layer parameters aside from the HK, HANI, and HFB parameters in the Strawberry Creek watershed. Values for HK ranged from 0.0001 ft/d along larger faults to 5.0000 ft/d for fault L-3 (fig. 12*A*). The model area was assumed to have dense fracturing and high anisotropy, which made the HK higher along rows than along columns. HANI ranged from 0.0001 to 0.1 with the lowest values assigned to faults and the rest of the area assigned approximately 0.1 (fig. 12*B*). In addition, HFBs that simulated faults were assigned the same HYDCHR used in layer 1 for layers 2 and 3 (fig. 12*C*). Specific storage (SS) had little effect on the model flow and hydraulic head because there were no layers specified as confined. If a layer is not confined, MODFLOW will not use the SS, but a value for the parameter must be provided. Therefore, both subbasins on the south side of the range were assigned a value of 0.000001, and the north side was assigned 0.0001 (fig. 12*D*).

Calibration Results

The results of the calibration for each spring diversion and the total of all spring diversions are plotted on figure 3. The annual reported flow for each spring diversion is plotted with the simulated annual flow. The mean flows for the historical period are plotted as horizontal dashed lines and annotated on the plots. The difference between the mean flows was the error in calibration. The best calibration was for Spring 1 and Spring 7 (figs. 3*A*, 3*D*), and the worst calibrations were for Tunnels 2 and 3, and the lower spring complex (figs. 3*B*, 3*C*, 3*E*). Tunnels 2 and 3 had simulated flow less than the reported flow, and the difficulty in calibration was primarily because the tunnels are so short that the model discretization caused all flow to springs to come from a single cell, which could not simulate the local geological complexity. The lower spring complex had simulated flow that was slightly higher than recorded. The result was that the error in the individual springs balanced the flow so that the mean flow was 0.2326 ft^3/s, which is 0.0314 ft^3/s, or 12 percent, less than the mean reported flow of 0.264 ft^3/s.

Simulated hydraulic heads are plotted with measured groundwater levels on figure 13 with the linear regression line. The higher elevation measurements are along the San Bernardino Mountains range crest, or on the north side of the model area, and the low elevation measurements are wells near the south end of the East Twin Creek watershed. The root mean square error (RMSE) of the difference between measured and simulated hydraulic heads was approximately 145.5 ft. The simulated hydraulic heads for wells closest to the upper Strawberry Creek watershed with groundwater-level measurements (02N04W25H, 02N03W30E3, and 02N03W30; fig. 1) were closer to the measured groundwater levels and had an RMSE of 38.9 ft.

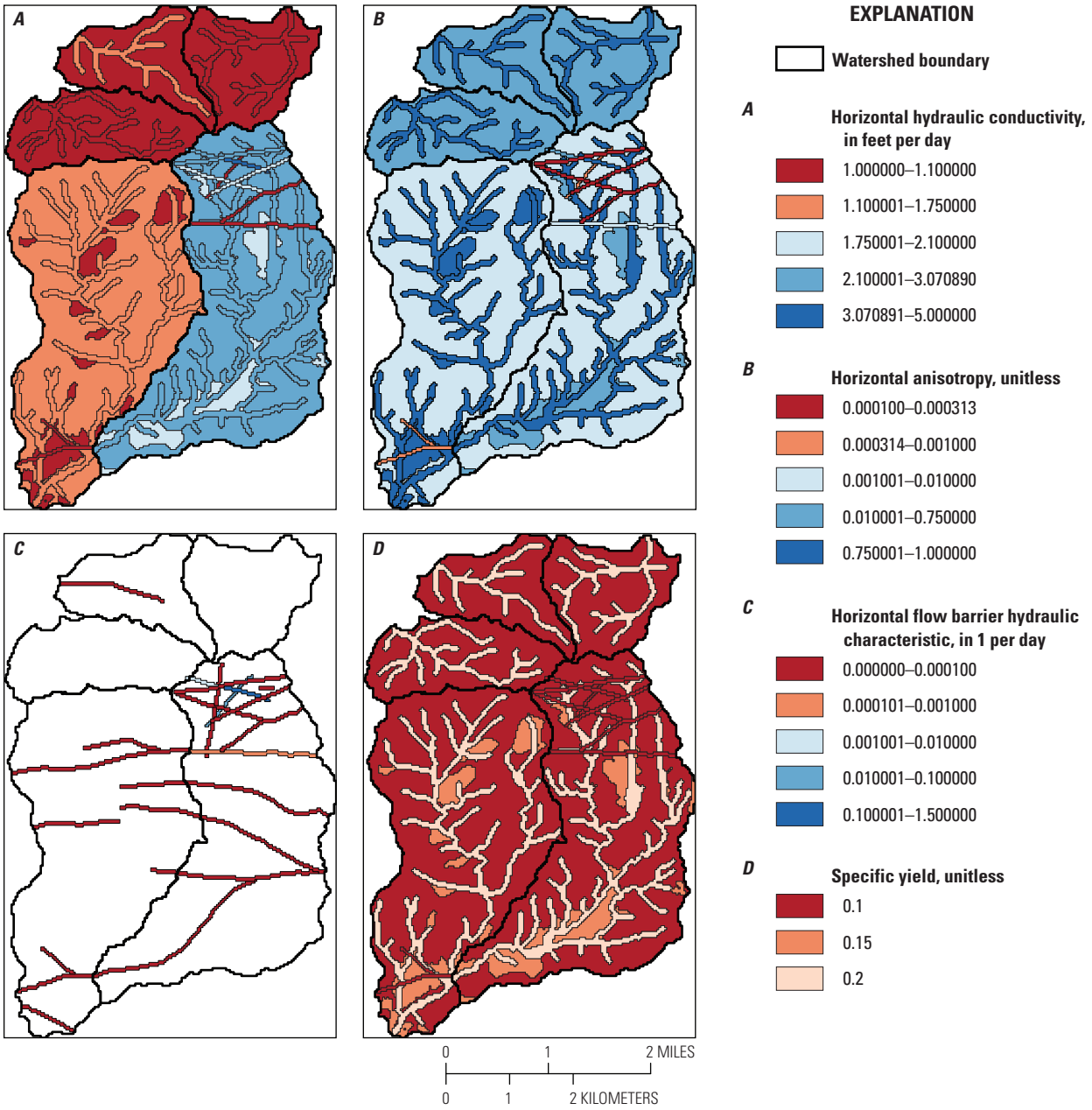


Figure 11. Model layer 1 hydraulic parameters zones and calibrated values for *A*, horizontal hydraulic conductivity (HK); *B*, HK anisotropy (HANI); *C*, horizontal flow barrier (HFB) hydraulic characteristic (HYDCHR); and *D*, specific yield (SY) parameters used in the Strawberry Creek Integrated Hydrological Model (Ryter, 2025), San Bernardino County, California.

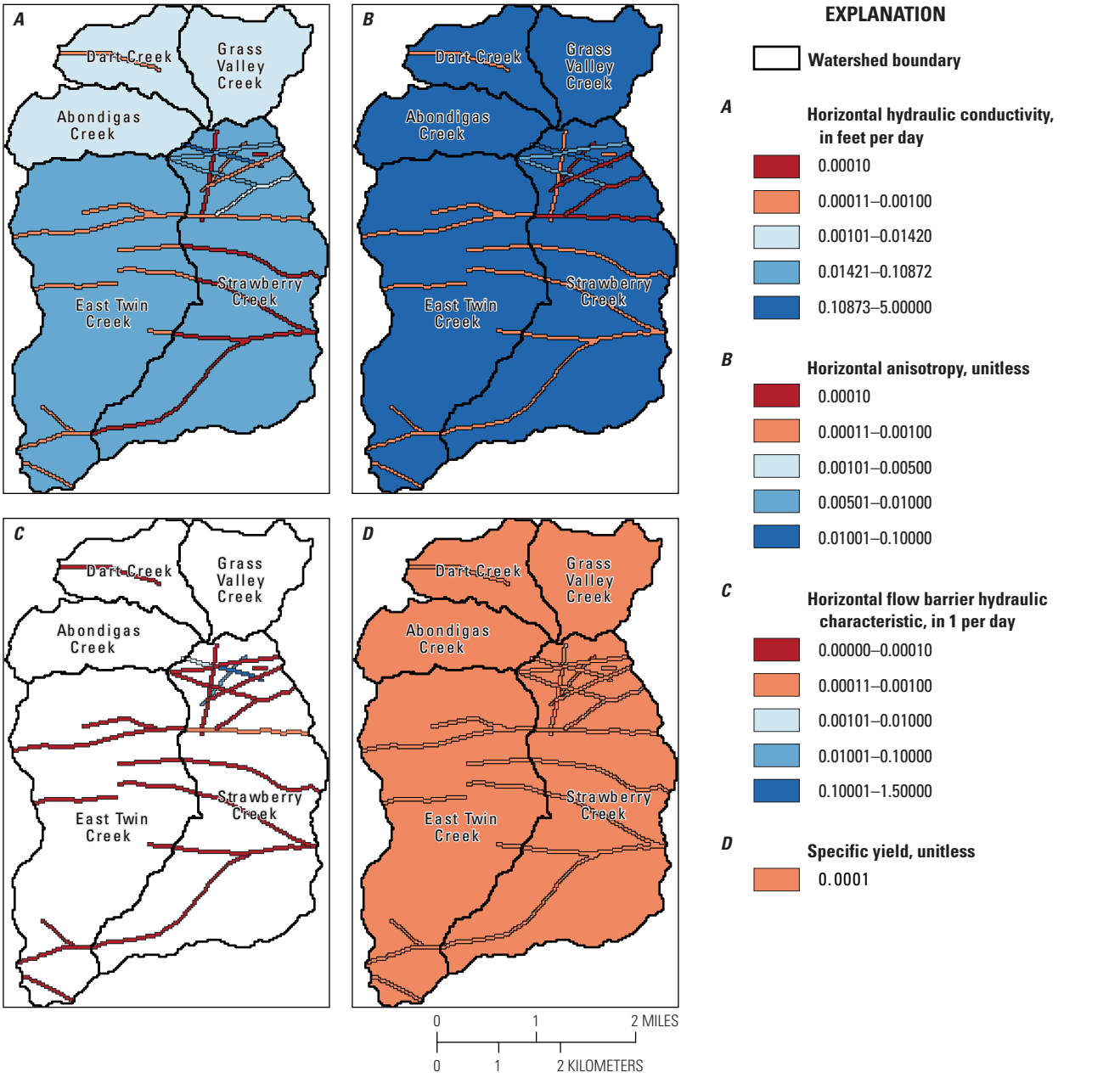


Figure 12. Layer 2 calibrated hydraulic parameters zones and calibrated values for *A*, horizontal hydraulic conductivity (HK); *B*, HK anisotropy (HANI); *C*, horizontal flow barrier (HFB) hydraulic characteristic (HYDCHR); and *D*, specific yield (SY) parameters used in the Strawberry Creek Integrated Hydrological Model (Ryter, 2025), San Bernardino County, California.

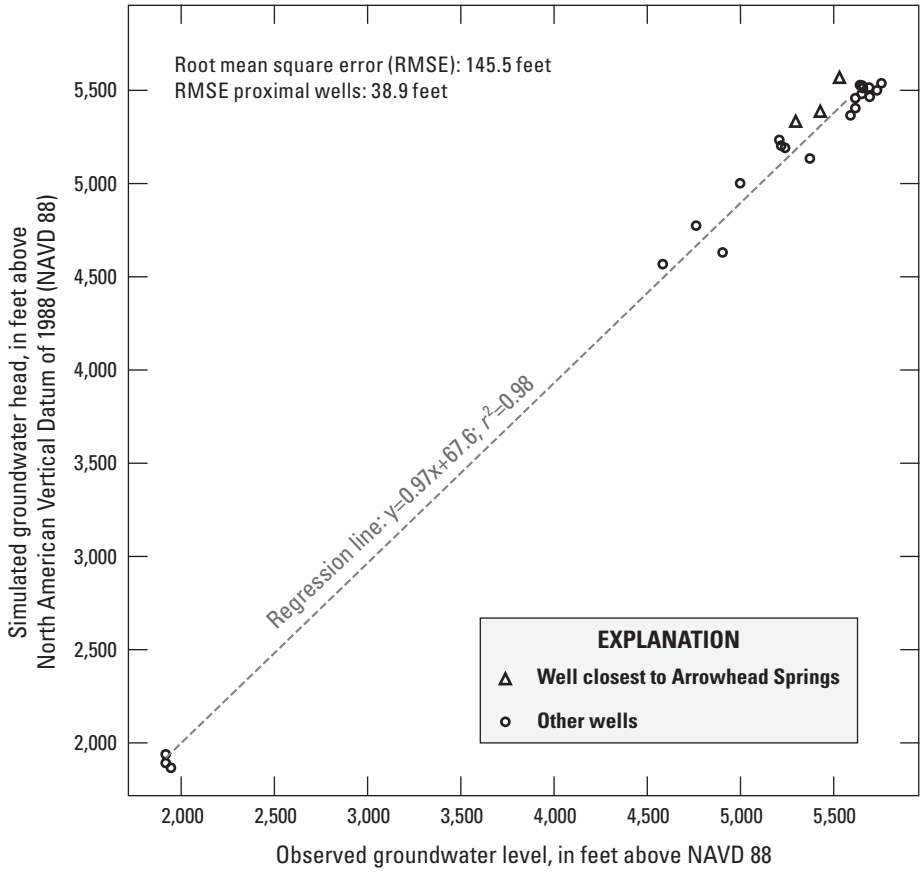


Figure 13. Observed groundwater levels and simulated hydraulic heads (Ryter, 2025) with a linear regression line, Strawberry Creek Integrated Hydrological Model, San Bernardino County, California.

Streamflow Capture by the Spring Diversion Structures

The SCIHM was run for the historical period without the spring diversions operating as a baseline model, and output was compared with the simulated streamflow with the diversions operating to determine the stream depletion by the diversion structures. Simulated streamflow data were extracted from the SCIHM at the SFR stream reach containing the confluence virtual gage (fig. 1), which is a location just upstream from east Strawberry Creek. That simulated flow represents the drainage affected by the spring diversions. Figure 14 shows time-series plots of the simulated spring diversion flow, the simulated streamflow with (affected) and without (baseline) diversions operating, stream loss caused by the spring diversions, and annual precipitation. Simulated streamflow was very erratic, with periods of base flow punctuated by high precipitation and large streamflow events (fig. 14*B*). Spring diversion flow increased after large runoff events. Simulated baseline streamflow followed the pattern of spring diversion flow and had a higher mean streamflow because of runoff events. However, the simulated streamflow affected by spring diversions operating in fig. 14*B* had much lower flow between runoff events, showing the effects of groundwater capture reducing base flow. The capture of groundwater from stream base flow was analyzed using the mean simulated baseline streamflow (0.38 ft^3/s), mean affected streamflow (0.28 ft^3/s), and mean simulated spring diversion flow (0.22 ft^3/s).

Stream loss here is defined as the baseline streamflow minus the affected streamflow. Stream loss is plotted on figure 14*C*. The mean stream loss was calculated by taking the difference between the mean baseline streamflow and the mean affected streamflow, which resulted in a mean stream loss of 0.10 ft^3/s. The plot of stream loss follows the trend of the spring diversion flow, showing that when there is more groundwater available, more is discharged from diversions, resulting in more capture of the streamflow. The ratio of stream loss to groundwater extraction by spring diversion structures, or stream-depletion factor (SDF), was 0.10 divided by 0.22, which equals 0.45. Approximately 45 percent of the spring-diversion extraction came from stream base flow. This value could have been higher except that there were long periods when capture caused Strawberry Creek to have no flow, so no more could be captured.

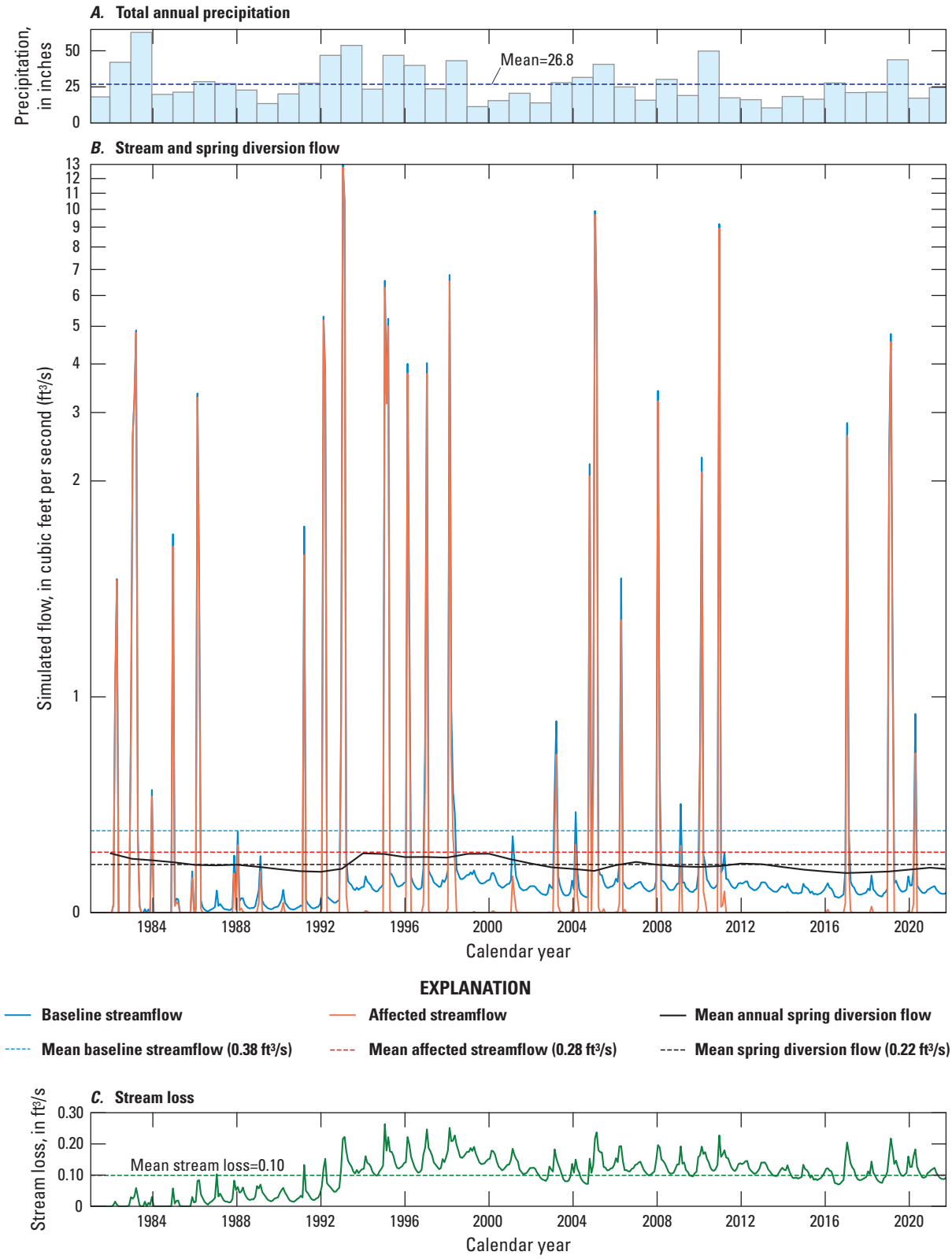


Figure 14. *A*, total annual precipitation and *B*, time-series plots of simulated mean monthly streamflow with and without spring diversions operating, and mean annual spring diversion flow (affected and baseline streamflow, respectively); and *C*, stream loss time series and mean stream loss for Strawberry Creek at the location referred to as the confluence virtual gage, Strawberry Creek Integrated Hydrological Model (Ryter, 2025), San Bernardino County, California. Figure 14*B* is a semi-log scale.

Discussion and Conclusions

The SCIHM shows the interplay between precipitation, temperature, aquifer recharge, streamflow, and spring diversion flow. The SCIHM simulated the very complex hydrogeology of the Arrowhead Springs area, and with climate inputs, quantified the effects of spring diversions.

Although diversions do not extract large volumes of water, they can still have substantial effects on streamflow in low-discharge headwater watersheds. Because spring diversions compete with streams for base flow, the loss of streamflow can be most detrimental during the dry season when most of the streamflow consists of base flow. This study indicated that 44 percent of the spring diversion flow came from base flow during the historical period. During wet periods, recharge and groundwater head increased, resulting in higher spring diversion flow and stream loss.

The mechanisms for stream depletion can be seen in the flow between groundwater and streams on figure 2*B*, where stream loss is symbolized as gaining base flow or losing flow to groundwater. Streams gain water upstream from faults and lose water on the downstream side. Spring diversion structures penetrate the aquifer upgradient of faults and access groundwater at the same locations where streams are gaining groundwater.

This study shows the hydrogeology and groundwater flow to springs in the semiarid San Bernardino Mountains and the effects of changes in precipitation and water extraction on streamflow in the headwaters of Strawberry Creek. The spring diversion structures extract groundwater from the same locations where base flow and natural springs, which once fed streams, have been replaced by these diversions. This change mostly affects streamflow during the dry season when there is little runoff and streamflow is mostly base flow. Simulation results showed that the capture of groundwater by spring diversions caused Strawberry Creek to have no flow for many dry seasons. Although the upper Strawberry Creek watershed provides low streamflow to lower parts of the watershed, base flow during the semiarid dry season can help support riverine habitats. Because of the low streamflow, it is very sensitive to groundwater extraction that results in stream base flow capture.

Model Limitations

The limited subsurface hydrogeological information mandated numerous assumptions about the groundwater model structure, making this model very approximate. Because of very little subsurface information, MODFLOW model layers were somewhat arbitrary. There was also little information on groundwater levels in the Strawberry Creek area and no useable local streamflow measurements. Finally, the reported spring diversion flow data were not necessarily representative of free-flowing drains and thus may not be as sensitive to changes in recharge and hydraulic head as they could be. This limitation causes the model results to be approximate because of limitations in the model calibration. Although the SCIHM provides an important tool for managing the streamflow and habitats in the Strawberry Creek watershed, the hydrogeological conceptualization could be improved with more hydrogeological and hydrological data.

Summary

To estimate the effects of spring diversion structures on headwater streamflow in the Strawberry Creek watershed, the Strawberry Creek Integrated Hydrological Model was constructed for the Strawberry Creek and adjacent East Twin Creek, Dart Creek, Abondigas Creek, and Grass Valley Creek watersheds. These watersheds are in the San Bernardino Mountains just east of the city of San Bernardino, California. The study area has about 4,900 feet (ft) of physical relief, rising from about 1,200 ft above the North American Vertical Datum of 1988 (NAVD 88) at the base of the range front on the south, to about 6,100 ft above NAVD 88 at Strawberry Peak. Elevation of the Arrowhead Springs local area, in the upper west branch subdrainage, ranges from about 4,150 to 5,330 ft above NAVD 88.

The hydrogeology of the study area consists of surficial deposits overlying fractured bedrock. Surficial deposits are decomposed granite bedrock, alluvium, and landslide deposits estimated to range from 20 to 180 ft thick. Fractured bedrock is assumed to become less fractured with depth and is broken into two layers. The top of layer 1 is the land surface. The thickness of the decomposed granite was set at 50 ft across the model except for the general Arrowhead Springs area, where the thickness was increased to as much as 500 ft, in essence combining the upper two layers so that the upper layer does not dry out where spring diversions are being simulated. Model layer 2 is the upper fractured bedrock zone with a thickness of 500 ft, and layer 3 is 984 ft thick.

Recharge is derived from land surface infiltration and stream leakage. Most recharge takes place in the upper elevations where precipitation is much more common. Aquifer discharge consists of base flow to streams, spring diversions, and well pumpage. Groundwater flows to the north and south away from the San Bernardino Mountains range crest and rises behind faults that act as horizontal flow barriers. In these areas, natural springs exist and streams gain base flow.

Downgradient from faults, streams lose flow to groundwater. Streamflow records at the East Twin Creek U.S. Geological Survey streamflow-gaging station were analyzed using base flow separation. Strawberry Creek and the adjacent East Twin Creek were found to be very dependent on base flow during the dry season (May–November), and the mean annual base-flow index, which is the fraction of the annual streamflow composed of base flow was 0.7.

The study area land cover is mostly mixed chaparral. Jeffrey pine is prevalent at the higher elevations, which receive more precipitation. The pines have deep roots that provide access to groundwater and increase evapotranspiration. Local areas of montane hardwood occur in all watersheds. The northern watersheds have a higher percentage of urban land cover, and the southern watersheds consist mostly of natural land cover because of the steep terrain. Land cover in the vicinity of the Arrowhead Springs is more variable and includes barren land as well as urban land cover upstream from the springs and montane hardwood downstream from the springs.

The Strawberry Creek Integrated Hydrological Model uses the coupled Groundwater and Surface-water Flow model, GSFLOW which is based on the integration of the precipitation-runoff modeling system PRMS and the modular groundwater flow model commonly called MODFLOW-2005. The PRMS model was calibrated to streamflow leaving the model area at the East Twin Creek streamflow-gaging station on the south, and Abondigas Creek streamflow-gaging station on the northwest side of the model. The MODFLOW model coupled with the PRMS model was calibrated to long-term average spring diversion flow. The model simulation period was 1981–2021.

The calibrated model was used to simulate Strawberry Creek streamflow with (affected) and without (baseline) the diversions operating to estimate the capture of streamflow by diversions in the headwaters of Strawberry Creek. The analysis estimated that about 45 percent of the water discharged by spring diversions came from Strawberry Creek. This study shows how the spring diversions extract groundwater from locations just upstream from natural springs, where streams receive base flow, thus having a direct effect on base flow and dry season streamflow.

References Cited

Albert A. Webb Associates, 2021, Crestline Village Water District 2020 urban water management plan: Crestline, Calif., Albert A. Webb Associates, 419 p., accessed December 18, 2024, at https://crestlinewater.specialdistrict.org/files/a20b11cc1/CVWD+UWMP+Final+2020.pdf.

Arguez, A., Durre, I., Applequist, S., Squires, M., Vose, R., Yin, X., and Bilotta, R., 2024, U.S. climate normals product suite (1981–2010): National Oceanic and Atmospheric Administration, National Centers for Environmental Information web page, accessed January 15, 2025, at https://doi.org/10.7289/V5PN93JP.

Barlow, P.M., and Leake, S.A., 2012, Streamflow depletion by wells—Understanding and managing the effects of groundwater pumping on streamflow: U.S. Geological Survey Circular 1376, 84 p., accessed November 21, 2024, at https://doi.org/10.3133/cir1376.

Bearmar, M., 2017, Geo-sciences specialist report—Reissuance of Nestle Waters North America special use permit: Report to the San Bernardino National Forest, 31 p.

Bense, V.F., Gleeson, T., Loveless, S.E., Bour, O., and Scibek, J., 2013, Fault zone hydrogeology: Earth-Science Reviews, v. 127, p. 171–192, accessed January 6, 2026, at https://doi.org/10.1016/j.earscirev.2013.09.008.

California Department of Forestry and Fire Protection, 2023, California vegetation—WHRTYPE: California Open Data Portal web page, accessed April 10, 2023, at https://data.ca.gov/dataset/california-vegetation-whrtype.

California Irrigation Management Information System, 2023, Potential evapotranspiration data: California Department of Water Resources, California Irrigation Management Information System web page, accessed April 4, 2023, at https://cimis.water.ca.gov/WSNReportCriteria.aspx.

Daly, C., Halbleib, M., Smith, J.I., Gibson, W.P., Doggett, M.K., Taylor, G.H., Curtis, J., and Pasteris, P.P., 2008, Physiographically sensitive mapping of climatological temperature and precipitation across the conterminous United States: International Journal of Climatology, v. 28, no. 15, p. 2031–2064, accessed January 6, 2026, at https://doi.org/10.1002/joc.1688.

Dames & Moore, Inc., 1999, Assessment of history and nature of Arrowhead Springs, San Bernardino Mountains, San Bernardino County, California: Rancho Cucamonda, Calif., Dames & Moore, Inc., Final Report, 160 p., accessed January 6, 2026, at https://www.waterboards.ca.gov/waterrights/water_issues/programs/enforcement/complaints/docs/investigation/6_fda_compliance_dames_moore_history.pdf.

Davis, S.N., 1969, Porosity and permeability of natural materials, *in* De West, R.J.M., ed., Flow through porous media: New York, Academic Press, p. 54–89.

Duan, Q., Yang, X., and Chen, J., 2017, Hydraulic properties of a low permeable rupture zone on the Yingxiu-Beichuan Fault activated during the Wenchuan earthquake, China—Implications for fluid conduction, fault sealing, and dynamic weakening mechanisms: Tectonophysics, v. 721, p. 123–142, accessed January 6, 2026, at https://doi.org/10.1016/j.tecto.2017.10.002.

Evans, J.P., Forster, C.B., and Goddard, J.V., 1997, Permeability of fault-related rocks, and implications for hydraulic structure of fault zones: Journal of Structural Geology, v. 19, no. 11, p. 1393–1404, accessed January 6, 2026, https://doi.org/10.1016/S0191-8141(97)00057-6.

Folch, A., and Mas-Pla, J., 2008, Hydrogeological interactions between fault zones and alluvial aquifers in regional flow systems: Hydrological Processes, v. 22, no. 17, p. 3476–3487, accessed January 6, 2026, at https://doi.org/10.1002/hyp.6956.

Freeze, R.A., and Cherry, J.A., 1979, Groundwater: Engelwood Cliffs, N.J., Prentice-Hall, Inc., 604 p.

Guzman, J.A., Moriasi, D.N., Gowda, P.H., Steiner, J.L., Starks, P.J., Arnold, J.G., and Srinivasan, R., 2015, A model integration framework for linking SWAT and MODFLOW: Environmental Modelling & Software, v. 73, p. 103–116, accessed January 6, 2026, at https://doi.org/10.1016/j.envsoft.2015.08.011.

Haley & Aldrich, Inc., 2022, Hydrologic characterization of surface water and groundwater resources, Strawberry Canyon, San Bernardino County, California: Report to the San Bernardino National Forest, 812 p.

Harbaugh, A.W., 2005, MODFLOW-2005—The U.S. Geological Survey modular ground-water model—The ground-water flow process: U.S. Geological Survey Techniques and Methods, book 6, chap. A16, variously paged, accessed January 6, 2026, at https://doi.org/10.3133/tm6A16.

Hevesi, J.A., and Johnson, T.D., 2016, Estimating spatially and temporally varying recharge and runoff from precipitation and urban irrigation in the Los Angeles Basin, California: U.S. Geological Survey Scientific Investigations Report 2016–5068, 192 p., accessed January 6, 2026, at https://doi.org/10.3133/sir20165068.

Jensen, M.E., and Haise, H.R., 1963, Estimating evapotranspiration from solar radiation: Journal of the Irrigation and Drainage Division, v. 89, no. 4, p. 15–41, accessed January 6, 2026, at https://doi.org/10.1061/JRCEA4.0000287.

Kneebone, W.R., Kopec, D.M. and Mancino, C.F., 1992, Water requirements and irrigation, chap. 12 *of* Waddington, D.V., Carrow, R.N., and Shearman, R.C., eds., Turfgrass: American Society of Agronomy, Crop Science Society of America, and Soil Science Society of America, v. 32, p. 441–472, accessed January 6, 2026, at https://doi.org/10.2134/agronmonogr32.c12.

Konikow, L.F., Hornberger, G.Z., Halford, K.J., Hanson, R.T., and Harbaugh, A.W., 2009, Revised multi-node well (MNW2) package for MODFLOW ground-water flow model: U.S. Geological Survey Techniques and Methods, book 6, chap. A30, 67 p., accessed January 6, 2026, at https://doi.org/10.3133/tm6A30.

Markstrom, S.L., Niswonger, R.G., Regan, R.S., Prudic, D.E., and Barlow, P.M., 2008, GSFLOW—Coupled ground-water and surface-water flow model based on the integration of the precipitation-runoff modeling system (PRMS) and the modular ground-water flow model (MODFLOW-2005): U.S. Geological Survey Techniques and Methods, book 6, chap. D1, 240 p., accessed January 6, 2026, at https://doi.org/10.3133/tm6D1.

Markstrom, S.L., Regan, R.S., Hay, L.E., Viger, R.J., Webb, R.M., Payn, R.A., and LaFontaine, J.H., 2015, PRMS-IV, the precipitation-runoff modeling system, version 4: U.S. Geological Survey Techniques and Methods, book 6, chap. B7, 158 p., accessed January 6, 2026, at https://doi.org/10.3133/tm6B7.

Mayer, A., May, W., Lukkarila, C., and Diehl, J., 2007, Estimation of fault-zone conductance by calibration of a regional groundwater flow model—Desert Hot Springs, California: Hydrogeology Journal, v. 15, p. 1093–1106, accessed January 6, 2026, at https://doi.org/10.1007/s10040-007-0158-0.

Meyer, J.L., Strayer, D.L., Wallace, J.B., Eggert, S.L., Helfman, G.S., and Leonard, N.E., 2007, The contribution of headwater streams to biodiversity in river networks: Journal of the American Water Resources Association, v. 43, no. 1, p. 86–103, accessed January 6, 2026, at https://doi.org/10.1111/j.1752-1688.2007.00008.x.

Morton, D.M., and Miller, F.K., 2006, Geologic map of the San Bernardino and Santa Ana 30’ x 60’ quadrangles, California: U.S. Geological Survey Open-File Report 2006–1217, 194 p., accessed January 6, 2026, at https://doi.org/10.3133/ofr20061217.

Nash, J.E., and Sutcliffe, J.V., 1970, River flow forecasting through conceptual models part I—A discussion of principles: Journal of Hydrology, v. 10, no. 3, p. 282–290, accessed January 6, 2026, at https://doi.org/10.1016/0022-1694(70)90255-6.

Niswonger, R.G., Panday, S., and Ibaraki, M., 2011, MODFLOW-NWT, a Newton formulation for MODFLOW-2005: U.S. Geological Survey Techniques and Methods, book 6, chap. A37, 44 p., accessed November 4, 2024, at https://doi.org/10.3133/tm6A37.

Niswonger, R.G., and Prudic, D.E., 2005, Documentation of the streamflow-routing (SFR2) package to include unsaturated flow beneath streams—A modification to SFR1: U.S. Geological Survey Techniques and Methods, book 6, chap. A13, 51 p., accessed January 6, 2026, at https://doi.org/10.3133/tm6A13.

PRISM Climate Group, 2020, PRISM weather data: Oregon State University Northwest Alliance for Computational Science and Engineering database, accessed December 15, 2020, at https://prism.oregonstate.edu.

Roy, J.W., Zaitlin, B., Hayashi, M., and Watson, S.B., 2011, Influence of groundwater spring discharge on small-scale spatial variation of an alpine stream ecosystem: Ecohydrology, v. 4, no. 5, p. 661–670, accessed January 6, 2026, at https://doi.org/10.1002/eco.156.

Ryter, D., 2025, Integrated hydrological model for simulating the impacts of spring diversions on streamflow in the Strawberry Creek watershed, San Bernardino County, California: U.S. Geological Survey data release, at https://doi.org/10.5066/P13AN2RJ.

Siade, A.J., Nishikawa, T., Rewis, D.L., Martin, P., and Phillips, S.P., 2014, Groundwater-flow and land-subsidence model of Antelope Valley, California: U.S. Geological Survey Scientific Investigations Report 2014–5166, 138 p., accessed January 6, 2026, at https://doi.org/10.3133/sir20145166.

Sloto, R.A., and Crouse, M.Y., 1996, HYSEP—A computer program for streamflow hydrograph separation and analysis: U.S. Geological Survey Water-Resources Investigation Report 96–4040, 46 p., accessed January 6, 2026, at https://doi.org/10.3133/wri964040.

Springer, A.E., Stevens, L.E., Ledbetter, J.D., Schaller, E.M., Gill, K.M., and Rood, S.B., 2015, Ecohydrology and stewardship of Alberta springs ecosystems: Ecohydrology, v. 8, no. 5, p. 896–910, accessed January 6, 2026, at https://doi.org/10.1002/eco.1596.

U.S. Department of Agriculture, 2003, Web soil survey: U.S. Department of Agriculture, Natural Resources Conservation Service web page, accessed November 15, 2003, at https://websoilsurvey.nrcs.usda.gov/.

U.S. Geological Survey, 2024, USGS water data for the Nation: U.S. Geological Survey National Water Information System database, accessed December 18, 2024, at https://doi.org/10.5066/F7P55KJN.

Western Regional Climate Center, 2023, Squirrel Inn 1, California (048476): Western Regional Climate Center web page, accessed May 15, 2024, at https://wrcc.dri.edu/cgi-bin/cliMAIN.pl?ca8476.

Western-San Bernardino Watermaster, 2023, Annual reports of the Western-San Bernardino Watermaster: Western-San Bernardino Watermaster web page, v. 1–8, accessed December 9, 2023, at https://westernwaterca.gov/204/Watermaster-Reports.

Wibberley, C.A.J., and Shimamoto, T., 2003, Internal structure and permeability of major strike-slip fault zones—The Median Tectonic Line in Mie Prefecture, southwest Japan: Journal of Structural Geology, v. 25, no. 1, p. 59–78, accessed January 6, 2026, at https://doi.org/10.1016/S0191-8141(02)00014-7.

Zhen, L., and Martin, P., 2011, Geohydrology, simulation of regional groundwater flow, and assessment of water management strategies, Twentynine Palms area, California: U.S. Geological Survey Scientific Investigations Report 2010–5249, 90 p., accessed January 6, 2026, at https://doi.org/10.3133/sir20105249.

For more information concerning the research in this report, contact the

Director, California Water Science Center
U.S. Geological Survey
6000 J Street, Placer Hall
Sacramento, California 95819
https://www.usgs.gov/centers/california-water-science-center

Publishing support provided by the USGS Science Publishing Network,
Sacramento Publishing Service Center

ISSN 2328-0328 (online)
https://doi.org/10.3133/sir20265040
Supersedes preprint
https://doi.org/10.31223/X5JB2K